Accepted Manuscript

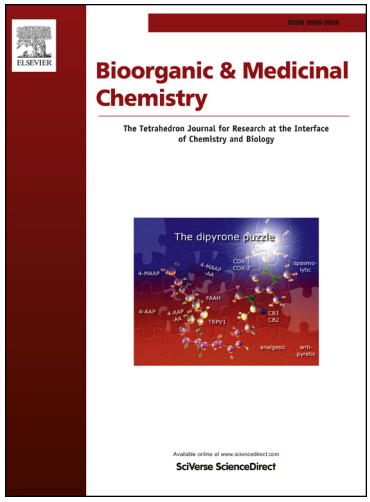

Structure Activity Relationships of Benzyl C-region Analogues of 2-(3-Fluoro-4-methylsulfonamidophenyl) propanamides as Potent TRPV1 Antagonists

Jihyae Ann, Aeran Jung, Mi-Yeon Kim, Hyuk-Min Kim, HyungChul Ryu, Sunjoo Kim, Dong Wook Kang, Sunhye Hong, Minghua Cui, Sun Choi, Peter M. Blumberg, Robert Frank-Foltyn, Gregor Bahrenberg, Hannelore Stockhausen, Thomas Christoph, Jeewoo Lee

PII: S0968-0896(15)30079-1
DOI: http://dx.doi.org/10.1016/j.bmc.2015.10.001
Reference: BMC 12601

To appear in: *Bioorganic & Medicinal Chemistry*

Received Date: 5 September 2015
Revised Date: 30 September 2015
Accepted Date: 1 October 2015

Please cite this article as: Ann, J., Jung, A., Kim, M-Y., Kim, H-M., Ryu, H., Kim, S., Kang, D.W., Hong, S., Cui, M., Choi, S., Blumberg, P.M., Frank-Foltyn, R., Bahrenberg, G., Stockhausen, H., Christoph, T., Lee, J., Structure Activity Relationships of Benzyl C-region Analogues of 2-(3-Fluoro-4-methylsulfonamidophenyl) propanamides as Potent TRPV1 Antagonists, *Bioorganic & Medicinal Chemistry* (2015), doi: http://dx.doi.org/10.1016/j.bmc.2015.10.001

Structure Activity Relationships of Benzyl C-region Analogues of 2-(3-Fluoro-4-methylsulfonamidophenyl) propanamides as Potent TRPV1 Antagonists

Jihyae Ann [a], Aeran Jung [a], Mi-Yeon Kim [a], Hyuk-Min Kim [a], HyungChul Ryu [b], Sunjoo Kim [b], Dong Wook Kang [c], Sunhye Hong [d], Minghua Cui [d], Sun Choi [d], Peter M. Blumberg [e], Robert Frank-Foltyn [f], Gregor Bahrenberg [f], Hannelore Stockhausen [f], Thomas Christoph [f], Jeewoo Lee [a,*]

[a] Laboratory of Medicinal Chemistry, Research Institute of Pharmaceutical Sciences, College of Pharmacy, Seoul National University, Seoul 151-742, Korea

[b] J2H Biotech, Ansan-si, Gyeonggi-do, Korea

[c] Department of Pharmaceutical Science and Technology, College of Health and Medical Science, Catholic University of Deagu, Gyeongsan-si, Gyeongsangbuk-do 712-702, Korea

[d] National Leading Research Laboratory of Molecular Modeling & Drug Design, College of Pharmacy, Graduate School of Pharmaceutical Sciences, and Global Top 5 Research Program, Ewha Womans University, Seoul 120-750, Korea

[e] Laboratory of Cancer Biology and Genetics, Center for Cancer Research, National Cancer Institute, NIH, Bethesda, MD 20892, USA

[f] Grünenthal Innovation, Grünenthal GmbH, D-52078 Aachen, Germany

** To whom correspondence should be addressed.*

Phone: 82-2-880-7846

Fax: 82-2-888-0649

E-mail: *jeewoo@snu.ac.kr*

Key Words: Vanilloid Receptor 1, TRPV1 antagonists, analgesic

Abstract

A series of 2-substituted 4-(trifluoromethyl)benzyl C-region analogues of 2-(3-fluoro-4-methylsulfonamidophenyl)propanamides were investigated for *h*TRPV1 antagonism. The analysis indicated that the phenyl C-region derivatives exhibited better antagonism than those of the corresponding pyridine surrogates for most of the series examined. Among the phenyl C-region derivatives, the two best compounds **43** and **44*S*** antagonized capsaicin selectively relative to their antagonism of other activators and showed excellent potencies with $K_{i(\mathrm{CAP})}$ = 0.3 nM. These two compounds blocked capsaicin-induced hypothermia, consistent with TRPV1 as their site of action, and they demonstrated promising analgesic activities in a neuropathic pain model without hyperthermia. The docking study of **44*S*** in our *h*TRPV1 homology model indicated that its binding mode was similar with that of its pyridine surrogate in the A- and B-regions but displayed a flipped configuration in the C-region.

1. Introduction

Despite its great medical importance, therapeutic approaches for treatment of pain remain limited. Recently, TRPV1 has emerged as a promising new target.[1-3] TRPV1 is a key nociceptor integrating direct inputs including low pH, elevated temperature, or chemicals such as capsaicin, along with indirect inputs routed through signaling pathways such as that of protein kinase C. Starting with structures of lead agonists such as capsaicin[4] and resiniferatoxin,[5] intense medicinal chemistry efforts are yielding potent antagonists along with better understanding of TRPV1 pharmacology.[6] A key finding is that compounds may have different antagonistic activities, both in terms of their efficacy and potency, for different TRPV1 activators.[7-8] An obstacle to the clinical development of TRPV1 antagonists that emerged with the first generation of antagonists was their induction of hyperthermia *in vivo*. Compounds with selective antagonism, blocking activation by capsaicin but not low pH, show initial promise of circumventing this problem.[8] Here, we describe our on-going exploration of the structure activity relations for *h*TRPV1 antagonists and the detailed characterization of lead compounds for selective antagonism against various activators and for *in vivo* activity.

Recently, we demonstrated that a series of *N*-{(6-trifluoromethyl-pyridin-3-yl)methyl} 2-(3-fluoro-4-methylsulfonamidophenyl)propanamides were potent *h*TRPV1 antagonists for multiple activators.[9-13] The antagonistic template can be divided into three pharmacophoric parts, designated as the A, B and C-regions, and was initially designed by the pharmacophoric combination of the A and C-regions of previous leads (**Figure 1**). The analysis of the structure activity relationship of the template initially focused on the pyridine C-region in which the 2-substituent was extensively explored by incorporating a variety of functional groups, including amino,[9] oxy,[10] thio,[11] alkyl[12] and aryl[13] groups. In addition, the 6-trifluoromethyl was replaced with its isosteres and the pyridine was replaced with its isomers.[14] In these series, multiple compounds displayed highly potent and (*S*)-stereospecific antagonism of *h*TRPV1 activators including capsaicin, *N*-arachidonoyl dopamine (NADA), low pH, heat (45 ^{o}C). In addition, our *in vivo* analysis of promising candidates from the

above series confirmed that they all blocked capsaicin-induced hypothermia, consistent with their *in vitro* mechanism of action, and, most importantly, they displayed potent antiallodynic activities in neuropathic pain models. Molecular modeling using our established *h*TRPV1 homology model indicated that the 6-trifluoromethyl group and the 2-substituents in the C-region made hydrophobic interactions with the hydrophobic pockets composed of Leu547/Thr550 and Met514/Leu515, respectively, and were critical for the potent activity of the antagonists.

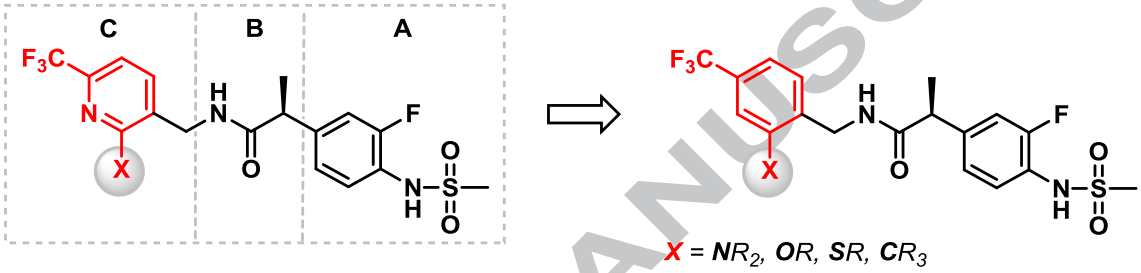

Figure 1. 4-(Trifluoromethyl)benzyl C-region TRPV1 antagonists

In continuation of our effort to further optimize the C-region as we seek to develop clinical candidates for neuropathic pain, we have investigated the phenyl surrogates of the selected pyridine C-region derivatives previously reported as potent antagonists (**Figure 1**).[9-13] As reported here, we synthesized a series of 2-substituted 4-(trifluoromethyl)benzyl C-region derivatives, we evaluated them for antagonism of *h*TRPV1 activation by multiple activators, and we compared their activities with those of the corresponding pyridine surrogates. With selected potent antagonists in the series, we further characterized their inhibition of capsaicin-induced hypothermia and their analgesic activity in animal models. Finally, we carried out a docking study with our *h*TRPV1 homology model to identify their binding mode to the receptor.

2. Result and discussion

2.1. Chemistry

A library of 4-(trifluoromethyl)benzonitriles (**4**) with various 2-substituents was synthesized starting from commercially available 2-chloro-4-(trifluoromethyl)benzonitrile (**2**) employing 6 different methods as appropriate. The benzonitriles (**4**) were reduced to the corresponding C-region amines by catalytic hydrogenation or with borane. The synthesized C-region amines were then coupled with propionic acid[9] as previously reported to afford the final compounds **7-62** (**Scheme 1**).

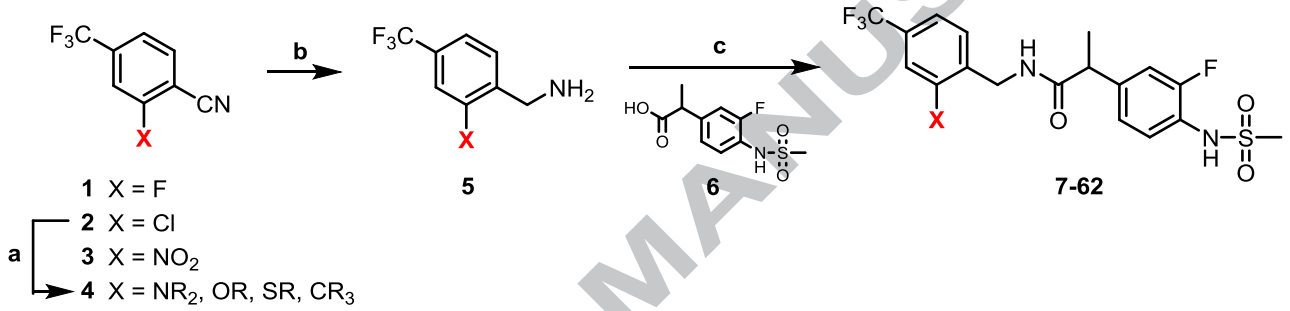

Scheme 1. General synthesis of 2-(3-fluoro-4-(methylsulfonamido)phenyl) propanamide analogues ***Reagents and conditions***: (a) [Method A] NR_2, DBU, 1,4-dioxane, 50 ºC, 12 h for **7-26**; [Method B] neat NR_2, DMF, 120 ºC, 6 h for **27**; [Method C] ROH, KO^{t}Bu, Toluene/DMBU, 70 ºC, 5 h for **28-35**; [Method D] neat ROH, DBU, 80 ºC, 3 h for **36, 37**; [Method E] RSH, K_2CO_3, 18-Crown-6, CH_3CN, reflux**,** 12 h for **38-49**; [Method F] R-$B(OH)_2$, $Pd(PPh_3)_4$, dppf, toluene/1,4-dioxane/2N Na_2CO_3, reflux, 12 h for **53-62**; (b) [Method G] H_2, 10% Pd-C, c-HCl, MeOH, 40 ºC, 8 h for **17, 27, 54**; [Method H] 2M $BH_3{\cdot}SMe_2$ in THF, reflux, 12 h for **7-16, 18-26**, **28-53, 55-62**; (c) EDC, HOBt, DMF, room temperature, 12 h.

2.2. *In vitro* Activity

The synthesized compounds were evaluated *in vitro* for TRPV1 antagonism as measured by inhibition of activation by capsaicin (100 nM). The assays were conducted using a fluorometric imaging plate reader (FLIPR) with human TRPV1 heterologously expressed in Chinese hamster ovary (CHO) cells.[9] The results are summarized in **Tables 1-4**. Comparison with the corresponding previously reported pyridine surrogates is presented in **Table 5**.[9-13]

First, we investigated the SAR for 2-amino derivatives (**Table 1**). Since the secondary amine derivatives of the pyridine C-region were found previously to be weak antagonists,[9] only ter-

tiary amine derivatives were investigated in this study. Among acyclic amine derivatives, the dipropylamine derivative (**8**) showed excellent antagonism with K_i = 0.3 nM. Among cyclic amine derivatives, 5 to 8-membered ring derivatives (**9**-**12**) exhibited similar antagonism around K_i = 2 nM. Since 4-substituted piperidinyl derivatives provided good antagonism in the pyridine C-region, their phenyl surrogates (**13**-**20**) were examined. As anticipated, they all displayed very potent antagonism with a range of K_i = 0.4-1.4 nM. In particular, the 4-trifluoromethyl (**16**) and the 4-(fluorobenzyl)piperidinyl (**19**-**20**) derivatives exhibited excellent antagonism with K_i = 0.4 nM. 4-Substituted piperazinyl derivatives were also examined. Most derivatives showed good antagonism except for the 4-cyclohexyl piperazinyl analog (**21**). The morpholine derivative (**27**) was found to be *ca.* 4-fold less potent than the corresponding piperidine surrogate (**10**).

Table 1. *In vitro h*TRPV1 antagonistic activities for 2-amino derivatives

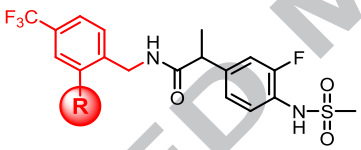

	R	K_i [CAP] (nM)		R	K_i [CAP] (nM)
7	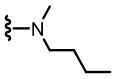	1.2	**18**	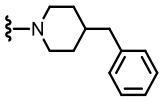	1.4
8	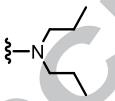	0.3	**19**	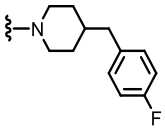	0.4
9		2.3	**20**	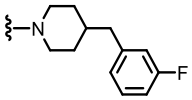	0.4
10		1.7	**21**	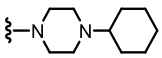	13.8
11		1.6	**22**	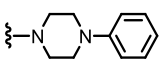	2.0
12	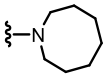	2.8	**23**	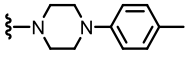	0.7
13	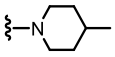	0.9	**24**	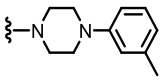	1.8

14	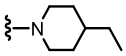	0.7	**25**	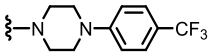	3.9
15	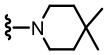	1.3	**26**	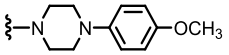	1.6
16	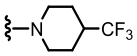	0.4	**27**		7.2
17	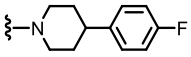	0.9			

Next, to investigate the SAR for 2-oxy derivatives of the phenyl C-region we began with the straight 2-alkyloxy derivatives (**Table 2**). Starting from the 2-propoxy derivative (**28**), the antagonistic activity was enhanced gradually as the number of carbons in the chain increased up to 5-6 carbons. The derivatives with 5-6 carbon chains (**30**, **31**) showed similar and potent antagonism with a range of K_i = 0.7-0.8 nM. The SAR of branched 2-alkyloxy and 2-cyclooxy derivatives was also investigated. The comparison of activity between straight and branched alkyl derivatives indicated that the branched alkyl derivatives generally showed slightly better antagonism than did the corresponding straight ones (*e.g.* **29** *vs.* **32**, **30** *vs.* **33**). A similar SAR pattern was examined in the comparison between straight and cyclic alkyl derivatives (*e.g.* **30** *vs.* **34**, **31** *vs.* **35**). The 2-benzyloxy derivatives were also investigated and were found to be potent antagonists. In particular, the 4-fluorobenzyloxy derivative (**37**) showed excellent antagonism with K_i = 0.5 nM.

Table 2. *In vitro h*TRPV1 antagonistic activities for 2-oxy derivatives

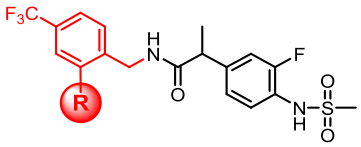

	R	K_i [CAP] (nM)		R	K_i [CAP] (nM)
28		2.0	**33**	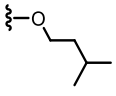	0.5

29	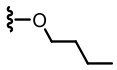	1.0	**34**		0.6
30	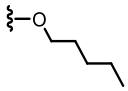	0.7	**35**		0.7
31	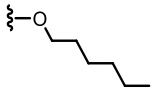	0.8	**36**	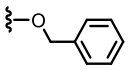	0.9
32		0.8	**37**	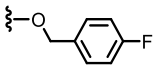	0.5

Next, we investigated the SAR for 2-thio derivatives of the phenyl C-region (**Table 3**). The SAR pattern was similar to that of the 2-oxy derivatives. The straight 2-alkylthio derivatives with 4 to 6 carbons in the chain showed potent, similar antagonism with a range of K_i = 1.8-2.3 nM. The comparison of activity between straight and branched/cyclic alkylthio derivatives indicated that the branched/cyclic alkylthio derivatives generally showed better antagonism than did the corresponding straight ones (*e.g.* **39** *vs.* **41**, **39** *vs.* **43** and **40** *vs.* **44**). In particular, the cyclopentylthio (**43**) and the cyclohexylthio (**44**) derivatives exhibited excellent antagonism with K_i = 0.3 and 0.5 nM, respectively. However, the incorporation of a polar group at the terminus of the 2-alkylthio group led to loss of activity as shown in **42**. The two stereoisomers of **44** were also examined and its *S*-isomer (**44*S***) showed marked stereospecific activity as previously reported and excellent antagonism with K_i = 0.3 nM.[3] In addition, we sought to evaluate the SAR of 2-benzylthio type derivatives since a series of the corresponding pyridine derivatives displayed potent antagonism. The 2-benzylthio derivative (**45**) exhibited outstanding antagonism with K_i = 0.5 nM, while its substituted derivatives (**46**-**48**) were found to be slightly less potent. The 2-(furan-2-yl)methylthio derivative (**49**) showed moderate antagonism.

Table 3. *In vitro h*TRPV1 antagonistic activities for 2-thio derivatives

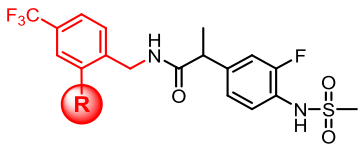

	R	K_i [CAP] (nM)		R	K_i [CAP] (nM)
38	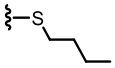	1.9	**44*S***	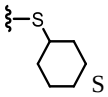	0.3
39	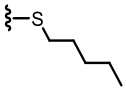	2.3	**44*R***	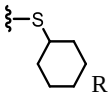	13.9
40	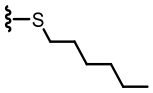	1.8	**45**	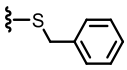	0.5
41	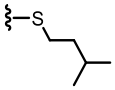	1.4	**46**	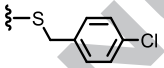	1.1
42	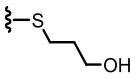	WE	**47**	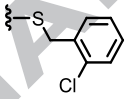	0.9
43		0.3	**48**	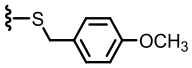	2.3
44		0.5	**49**	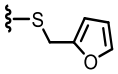	3.2

Finally, we investigated the SAR for 2-halo, nitro, alkyl and aryl derivatives of the phenyl C-region (**Table 4**). Although the 2-chloro derivative (**51**) showed good antagonism, the 2-fluoro (**50**) and 2-nitro (**52**) derivatives were found to be weak antagonists probably due to insufficient hydrophobic interactions with the receptor. Two representative 2-alkyl derivatives (**53**, **54**), selected from the 2-alkyl library of the pyridine C-region, exhibited excellent antagonism with K_i = 0.4 and 0.6 nM as expected. Substituted phenyl derivatives were also examined. Most phenyl derivatives showed outstanding antagonism with $K_i \approx 1$ nM except for the dimethoxy substituted phenyl derivatives (**60**, **61**). The 2-pyridine derivative (**62**) was found to be a weak antagonist.

Table 4. *In vitro h*TRPV1 antagonistic activities for 2-halo, alkyl and aryl derivatives

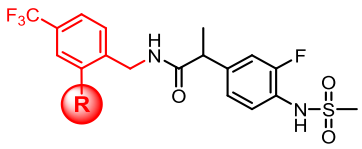

	R	K_i [CAP] (nM)		R	K_i [CAP] (nM)
50		68.7	**57**		1.9
51		4.0	**58**	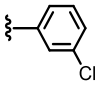	1.0
52		NE	**59**	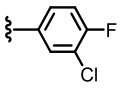	0.6
53	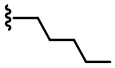	0.4	**60**	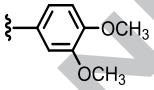	8.6
54		0.6	**61**	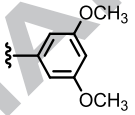	5.8
55	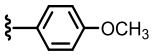	0.8	**62**		59.4
56	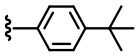	1.1			

In order to compare the potencies between corresponding phenyl and pyridine C-region derivatives, representative 2-substituted compounds were listed in **Table 5**. The SAR analysis indicated that whereas the pyridine derivatives showed better potency in the 2-amino series, the phenyl derivatives exhibited better potency in the 2-oxy and 2-thio series. The 2-alkyl and aryl series yielded mixed results.

Table 5. Comparison of *in vitro h*TRPV1 antagonistic activities for representative, corresponding antagonists from the pyridine and phenyl C-region series

	R	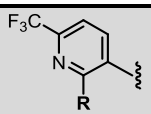	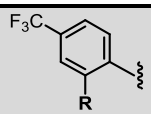
8		0.2	0.3

13	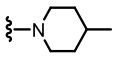	0.3	0.9
16	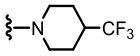	0.4	0.6
18	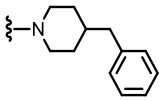	0.2	1.4
33	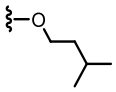	0.8	0.5
34		0.9	0.6
37	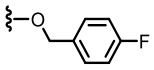	2.5	0.5
43		1.2	0.3
44		0.9	0.5
44*S*		0.4	0.3
47	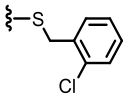	4.9	0.9
53	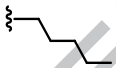	1	0.4
54		0.6	0.6
59	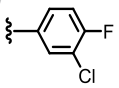	0.2	0.6

For detailed analysis of *in vitro* activities, the two most potent antagonists in this study, **43** and **44*S***, were investigated for other TRPV1 activators including low pH, heat (45 ^{o}C) and *N*-arachidonoyl dopamine (NADA) (**Table 6**). Whereas both antagonists showed excellent antagonism with subnanomolar potency toward capsaicin and NADA, they exhibited relatively lower po-

tency toward pH and heat. This selective pharmacological profile is thought to be promising for drug candidates.

Table 6. *In vitro h*TRPV1 antagonistic activities of **43** and **44*S*** for multiple activators.

Activators, parameter	**43**	**44*S***
CAP (f)K_i (nM)	0.3	0.3
NADA (f)K_i (nM)	0.03	0.03
pH, IC_{50} (nM)	32	20.4
heat 45^oC, IC_{50} (nM)	37.2	7.3

2.3. *In vivo* Activity

Consistent with its *in vitro* mechanism of action as an *h*TRPV1 antagonist, *in vivo* **43** and **44*S*** likewise blocked response to capsaicin (**Table 7**). Compounds were administered orally at a dose of 3 mg/kg 15 min before intraperitoneal injection of 3 mg/kg capsaicin following the procedure described previously.[1] This dose of **43** and **44*S*** inhibited the hypothermic response to capsaicin, assayed 30 min after capsaicin injection, by 80% and 57%, respectively. Compound **43** showed dose-dependent inhibition in capsaicin-induced hypothermia by 38% at a dose of 0.3 mg/kg. Importantly, both compounds by themselves did not show any hyperthermia at the given doses (data not shown).

Table 7. Inhibition of capsaicin-induced hypothermia after oral administration in the mouse. Data, n = 10, mean ± SEM, * $p<0.05$ vs vehicle.

Dose (mg/kg) /Inhibition %	0.3	3
CAP-induced Hypothermia		
43	38	80
44*S*	NT	57

We evaluated the *in vivo* analgesic activities of the above antagonists, **43** and **44*S***, upon oral administration in the Bennett mouse model of neuropathic pain (**Figure 2**). Both **43** and **44*S*** demonstrated dose-dependent antiallodynic efficacy in cold allodynia with max 48% and 57% MPE at 10 mg/kg, respectively. In addition both compounds were found to be thermoneutral in body temperature study.

Figure 2. Analgesic activity of compounds **43**, **44*S*** on CCI-induced cold allodynia (Bennett model) after oral administration in the mouse. Data, n = 10, mean ± SEM, * $p<0.05$ vs vehicle. MPE, maximal possible effect.

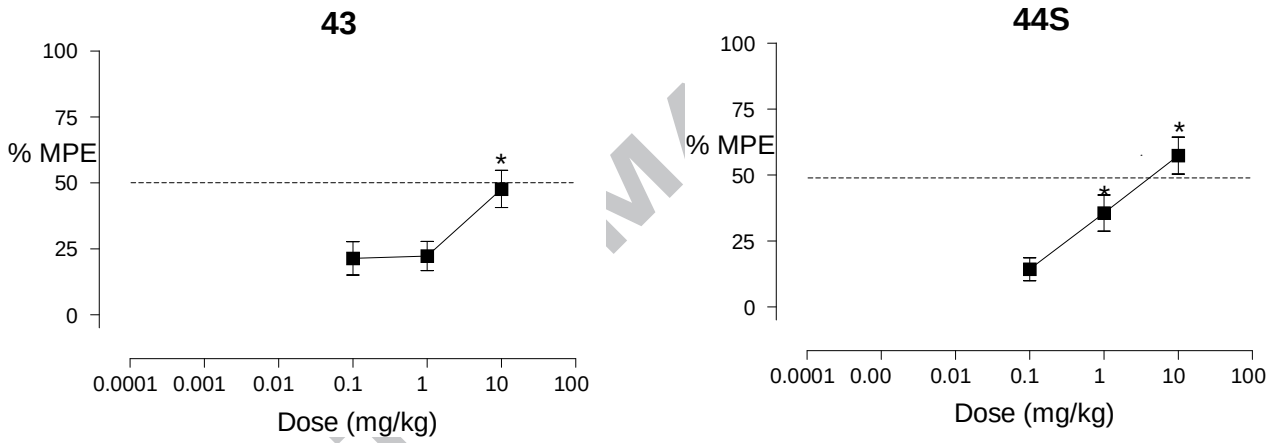

2.4. Molecular Modeling

To investigate the binding interactions of compound **44*S***, we performed a flexible docking study with our human TRPV1 (*h*TRPV1) model[9] generated based on our rat TRPV1 (*r*TRPV1) model.[7] Compared to the previously reported **24*S***,[11] the pyridine surrogate of **44*S***, only the pyridine ring is replaced by the phenyl ring in this compound. The binding modes of **44*S*** and **24*S***[11] appeared to be similar in the A- and B-regions. As shown in **Figure 3**, the methylsulfonamidophenyl group in the A-region fitted in the deep bottom hole and showed hydrophobic interactions with Tyr511, Ile564, and Ile569. Moreover, the sulfonamide NH formed a hydrogen bond with Ile564. The amide group in the B-region participated in hydrogen bonding with Tyr511, contributing to the proper po-

sitioning of the C-region for the hydrophobic interactions. In the C-region, the 2-cyclohexylthio group was expected to extend toward the hydrophobic region composed of Leu547 and Thr550 as did this group in **24*S***.[11] However, instead of the cyclohexyl ring, the 4-trifluoromethyl group was oriented toward the upper hydrophobic area and involved in the hydrophobic interaction with Leu515, Leu518, Leu547 and Thr550, along with Phe587 from the adjacent monomer. The absence of the pyridine nitrogen made this aromatic ring unable to form a hydrogen bond with Tyr511, which might have caused the flipped orientation of the two rings in the C-region compared with **24*S***.[11]

Figure 3. Docking result of **44*S*** in the *h*TRPV1 model.

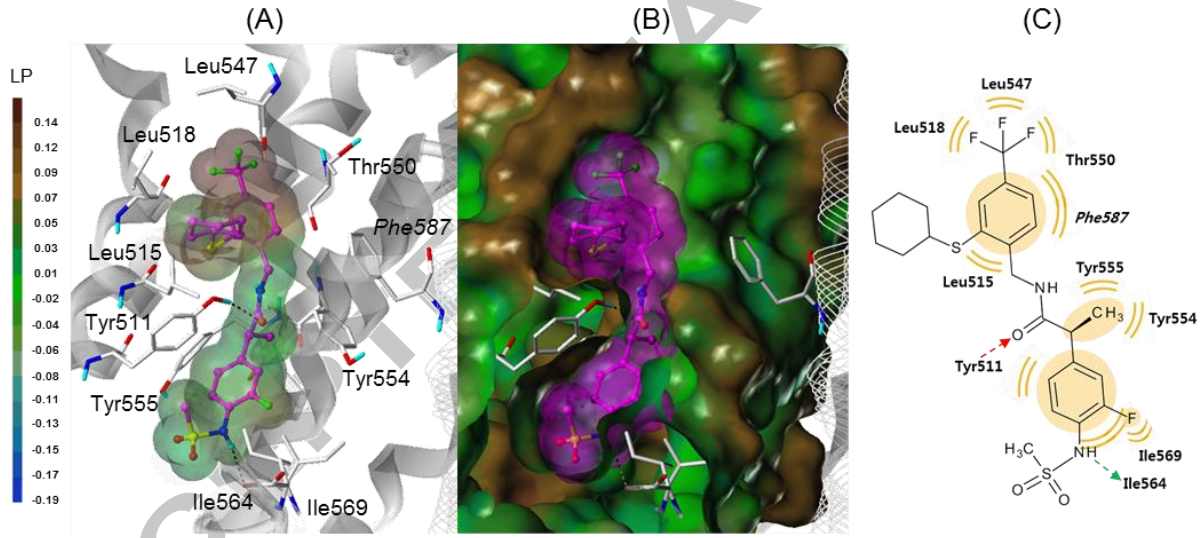

(A) Binding interactions of **44*S*** at the binding site of *h*TRPV1**.** The important interacting residues are labeled and shown as capped-stick with their carbon atoms in white color. The secondary structure of *h*TRPV1 is in gray color and the neighboring monomer helices are depicted in line ribbon. **44*S*** is displayed in ball-and-stick with the carbon atoms colored by magenta. The van der Waals surface of **44*S*** is shown by the lipophilic potential property. Hydrogen bonds are depicted as black dashed lines, and non-polar hydrogens are undisplayed for clarity. (B) The Fast Connolly surface of *h*TRPV1 and the van der Waals surface of the docked **44*S***. MOLCAD was used to generate the molecular surface of *h*TRPV1 and the surface is shown with the lipophilic potential property. For clarity, the surface of *h*TRPV1 is Z-clipped and that of the ligand is colored magenta. (C) 2-D representation of the interactions between **44*S*** and *h*TRPV1. Hydrophobic interactions are marked in light brown. Red and green arrows show the hydrogen bonding interactions with their directionality.

3. Conclusion

The structure activity relationship of 2-substituted 4-(trifluoromethyl)benzyl C-region analogues of 2-(3-fluoro-4-methylsulfonamidophenyl)propanamides was investigated for *h*TRPV1 antagonism and compared with that of the corresponding pyridine C-region surrogates previously reported. The analysis indicated that the phenyl C-region derivatives exhibited better antagonism than did the corresponding pyridine surrogates for most of the series. Among the compounds, the two best compounds, **43** and **44*S***, showed excellent antagonism toward capsaicin with $K_{i(CAP)}$ = 0.3 nM and marked selectivity for antagonism of capsaicin and NADA compared to that for low pH and heat. They blocked capsaicin-induced hypothermia, consistent with their actions *in vitro* being through TRPV1 and they demonstrated promising analgesic activities with 48% and 57% MPE, respectively, at 10 mpk in the neuropathic pain model. The docking study of **44*S*** in our *h*TRPV1 homology model indicated that its binding mode was similar with that of its pyridine surrogate in the A- and B-regions but displayed a flipped orientation of two hydrophobic groups in the C-region compared to its pyridine surrogate due to the absence of the pyridine nitrogen.

4. Experimental

4.1. Chemistry

4.1.1. General

All chemical reagents were commercially available. Melting points were determined on a Büchi Melting Point B-540 apparatus and are uncorrected. Silica gel column chromatography was performed on silica gel 60, 230-400 mesh, Merck. Nuclear magnetic resonance (^{1}H-NMR and ^{13}C-NMR) spectra were recorded on JEOL JNM-LA 300 [300 MHz (^{1}H), 75 MHz (^{13}C)] and Bruker Avance 400 MHz FT-NMR [400 MHz (^{1}H), 100 MHz(^{13}C)] spectrometers. Chemical shifts are reported in ppm units with Me_4Si as a reference standard. Infrared (IR) spectra were recorded on a JASCO FT/IR-4200 spectrometer. Mass spectra were recorded on a VG Trio-2 GC-MS and 6460 Triple Quad LC/MS. All final compounds were purified to >95% purity, as determined by

high-performance liquid chromatography (HPLC). HPLC was performed on an Agilent 1120 Compact LC (G4288A) instrument using an Agilent Eclipse Plus C18 column (4.6 x 250 mm, 5 μm) and a Daicel Chiralcel OD-H column (4.6 x 250 mm, 5 μm).

4.1.2. General Procedure for Amidation

4.1.2.1. Method A

A mixture of 2-chloro-4-(trifluoromethyl)-benzonitrile (1.00 mmol), appropriate amine (NR_2, 2.00 mmol), and DBU (2.5 mmol) were dissolved in 1,4-dioxane (8 ml). The mixture was stirred for 12 h at 50 °C. The reaction was quenched with water and extracted with EtOAc twice. The combined organic extracts were dried over $MgSO_4$, filtered, and concentrated *in vacuo*. The residue was purified by flash column chromatography on silica gel using EtOAc:hexane (1:7-1:10) eluant condition. (NR_2 = 4-(4-fluorophenyl)-1 2 3 6-tetrahydropyridine hydrochloride for **17**)

4.1.2.2. Method B

A mixture of 2-chloro-4-(trifluoromethyl)-benzonitrile (1.00 mmol), appropriate amine (NR_2, 2.00 mmol) were dissolved in DMF (8 ml). The mixture was stirred for 6 h at 120 °C. The reaction was quenched with water and extracted with EtOAc twice. The combined organic extracts were dried over $MgSO_4$, filtered, and concentrated *in vacuo*. The residue was purified by flash column chromatography on silica gel using EtOAc : hexane (1:7) eluant condition.

4.1.2.3. Method C

Appropriate ROH (3.00 mmol) was added to potassium *tert*-butoxide (3.00 mmol) solution in toluene (7 ml). 1,3-Dimethyl-3,4,5,6-tetrahydro-2(1H)-pyrimidinone (DMPU, 3 ml) was added to the mixture and stirred for 30 min at 80 °C. After cooled down to ambient temperature of the reaction mixture, 2-chloro-4-(trifluoromethyl)-benzonitrile (1.00 mmol) in toluene was dropwised and sttired for 3 h at 80°C. The reaction was quenched by adding water and extracted with with EtOAc

twice. The combined organic extracts were dried over $MgSO_4$, filtered, and concentrated *in vacuo*. The residue was purified by flash column chromatography on silica gel using EtOAc:hexane (1:7) eluant condition.

4.1.2.4. Method D

2-chloro-4-(trifluoromethyl)-benzonitrile (1.00 mmol) was dissolved in appropriate alcohol, and DBU (2.00 mmol) was added. The mixture was stirred for 3 h at 80 °C. The reaction was quenched with water and extracted with EtOAc twice. The combined organic extracts were dried over $MgSO_4$, filtered, and concentrated *in vacuo*. The residue was purified by flash column chromatography on silica gel using EtOAc : hexane (1:4) eluant condition.

4.1.2.5. Method E

A mixture of 2-chloro-4-(trifluoromethyl)-benzonitrile (1.00 mmol) and appropriate thiol (RSH, 3.00 mmol), 18-crown-6-ether (cat.) and potassium carbonate (2.00 mmol) were dissolved in acetonitrile (3 ml). The mixture was refluxed for 12 h and then cooled to ambient temperature. The mixture was quenched by adding water and extracted with EtOAc. Extracted organic compound was dried over $MgSO_4$, filtered, and concentrated *in vacuo*. The residue was purified by flash column chromatography on silica gel using EtOAc:hexane (1:4) eluant conditon. (RSH = $CH_3CO_2(CH_2)_2SH$ for **42**)

4.1.2.6. Method F

A mixture of 2-chloro-4-(trifluoromethyl)-benzonitrile (1.00 mmol), appropriate boronic acid (1.20 mmol) were dissolved in toluene:dioxane:2N Na_2CO_3 (2:1:1) solution (6 ml). Tetrakis(triphenyl-phosphine)palladium(0) (0.10 mmol) and 1,1′-Ferrocenediyl-bis(diphenylphosphine) (0.20 mmol) was added to the mixture and it was refluxed for 12 h. After cooled down to ambient temperature, the reaction was filtered over celite and

extracted with EtOAc twice. The combined organic extracts were dried over $MgSO_4$, filtered, and concentrated *in vacuo*. The residue was purified by flash column chromatography on silica gel using EtOAc : hexanes (1:10) eluant condition. ($R\text{-}B(OH)_2$ = 1-pentenyl boronic acid for **53**, 1-cyclohexenylboronicacid for **54**)

4.1.3. General Procedure for Nitrile Reduction

4.1.3.1. Method G

A suspension of nitrile compounds (1.00 mmol) and 10% Pd-C (20 mg/ mmol) and c-HCl (1 drop) in MeOH (3 ml) was charged with hydrogen gas for 6 h at room temperature and filtered through celite. The filtrate was concentrated *in vacuo*. The residue was purified by flash column chromatography on silica gel using MeOH:DCM (1:10) eluant condition.

4.1.3.2. Method H

To a stirred solution of nitrile (1.00 mmol) in anhydrous THF (10 ml) was added 2M $BH_3{\cdot}SMe_2$ in THF (1.1 mmol) at room temperature. After being refluxed for 8 h, the mixture was cooled to ambient temperature, 2 N HCl was dropwised, and the solution then refluxed for 30 min. After cooling to ambient temperature, the mixture was neutralized with 2 N NaOH and extracted with EtOAc several times. The combined organic layers were washed with brine, dried over $MgSO_4$, and concentrated *in vacuo*. The residue was purified by flash column chromatography on silica gel using MeOH:DCM (1:10) eluant condition.

4.1.4. General Procedure for Amide Coupling

A mixture of acid (1.00 mmol), amine (1.10 mmol), 1-(3-dimethylaminopropyl)-3-ethyl-carbodiimide hydrochloride (1.10 mmol) and 1-Hydroxybenzotriazole hydrate (1.50 mmol) in DMF (5 ml) was stirred for 12 h at room

temperature. The reaction mixture was extracted with EtOAc (10 ml). The aqueous phase was saturated with aq. NaCl and extracted again with EtOAc (15 ml). The combined organic extracts were washed with 1 N HCl (5 ml) and brine (5 ml), dried over $MgSO_4$, filtered, and concentrated *in vacuo*. The residue was purified by flash column chromatography on silica gel using EtOAc:hexanes (1:2) eluant condition.

4.1.4.1.

2-(3-Fluoro-4-(methylsulfonamido)phenyl)-N-(2-(butyl(methyl)amino)-4-(trifluorome-thyl)benzyl)propanamide (7).

Yield 55%, white solid, mp = 65-75 °C; ^{1}H NMR (300 MHz, $CDCl_3$) δ 7.52 (t, *J* = 8.25 Hz, 1H), 7.30 (s, 1H), 7.12 (m, 2H), 6.47 (m, 2H), 4.52 (m, 2H), 3.52 (d, *J* = 7.10 Hz, 1H), 3.01 (s, 3H), 2.08 (m, 2H), 2.60 (s, 3H), 1.52 (d, *J* = 7.14 Hz, 3H), 1.41 (m, 2H), 1.29 (m, 2H), 0.90 (t, *J* = 7.20 Hz, 3H); MS (FAB) *m/z* 504 (M+H).

4.1.4.2.

2-(3-Fluoro-4-(methylsulfonamido)phenyl)-N-(2-(dipropylamino)-4-(trifluoromethyl)-benzyl)propanamide (8).

Yield 60%, white solid, mp = 67 °C; ^{1}H NMR (300 MHz, $CDCl_3$) δ 7.52 (dd, *J* = 8.4, 8.4 Hz, 1H), 7.32 (s, 1H), 7.23-7.28 (m, 2H), 7.17 (dd, *J* = 11.2, 2.0 Hz, 1H), 7.09 (d, *J* = 8.3 Hz, 1H), 6.49 (bs, 1H), 6.36 (bt, 1H), 4.47-4.61 (m, 2H), 3.52 (q, *J* = 7.1 Hz, 1H), 3.03 (s, 3H), 2.79-2.90 (m, 4H), 1.52 (d, *J* = 7.1 Hz, 3H), 1.29-1.45 (m, 4H), 0.77-0.89 (m, 6H); MS (FAB) *m/z* 518 (M+H).

4.1.4.3.

2-(3-Fluoro-4-methanesulfonylamino-phenyl)-N-(2-pyrrolidin-1-yl-4-trifluoromethyl-benzyl)-propionamide (9).

Yield 70%, white solid, mp = 134 °C; ^{1}H NMR (300MHz, $CDCl_3$) δ 7.49 (t, *J* = 8.1 Hz, 1H),

7.05-7.19 (m, 5H), 6.79 (bs, 1H), 6.26 (bt, 1H), 4.49 (d, *J* = 4.8 Hz, 2H), 3.54 (q, *J* = 7.2 Hz, 1H), 3.08-3.12 (m, 4H), 3.01 (s, 3H), 1.86-1.90 (m, 4H), 1.50 (d, *J* = 7.2 Hz, 3H); MS (FAB) *m/z* 488 (M+H).

4.1.4.4.

2-(3-Fluoro-4-methanesulfonylamino-phenyl)-N-(2-piperidin-1-yl-4-trifluoromethyl-benzyl)-propionamide (10).

Yield 80%, pale yellow solid, mp = 68 °C; ^{1}H NMR (300MHz, $CDCl_3$) δ 7.48 (t, *J* = 8.3 Hz, 1H), 7.32 (bd, 2H), 7.05-7.15 (m, 4H), 6.81 (bs, 1H), 6.66 (bt, 1H), 4.52 (d, *J* = 5.1 Hz, 2H), 3.55 (q, *J* = 6.9 Hz, 1H), 3.00 (s, 3H), 2.79 (bs, 4H), 1.49-1.64 (m, 6H), 1.25 (m, 3H); MS (FAB) *m/z* 502 (M+H).

4.1.4.5.

2-(3-Fluoro-4-methanesulfonylamino-phenyl)-N-(2-azepan-1-yl-4-trifluoromethyl-benzyl)-propionamide (11).

Yield 58%, white solid, mp = 76-80 °C; ^{1}H NMR (300 MHz, $CDCl_3$) δ 7.51 (dd, *J* = 8.2, 8.2 Hz, 1H), 7.32 (s, 1H), 7.23 (s, 2H), 7.14 (dd, *J* = 11.3, 1.9 Hz, 1H), 7.08 (d, *J* = 8.2 Hz, 1H), 6.52 (bs, 1H), 6.43 (bt, 1H), 4.53 (m, 2H), 3.54 (q, *J* =7.0 Hz, 1H), 3.04-3.00 (m, 7H), 1.72-1.64 (m, 8H), 1.52 (d, *J* = 7.0 Hz, 3H); MS (FAB) *m/z* 516 (M+H).

4.1.4.6.

2-(3-Fluoro-4-methanesulfonylamino-phenyl)-N-(2-azocan-1-yl-4-trifluoromethyl-benzyl)-propion-amide (12).

Yield 48%, white solid, mp = 73 °C; ^{1}H NMR (300 MHz, $CDCl_3$) δ 7.52 (dd, *J* = 8.3, 8.3 Hz, 1H), 7.38 (s, 1H), 7.22-7.25 (m, 2H), 7.15 (dd, *J* = 11.2, 2.0 Hz, 1H), 7.11 (d, *J* = 8.1 Hz, 1H), 6.51 (bs, 1H), 6.01 (bt, 1H), 4.55 (d, *J* = 5.7 Hz), 3.55 (q, *J* = 7.5 Hz, 1H), 3.00-3.05 (m, 7H), 1.62-1.72 (m,

10H), 1.53 (d, *J* = 7.1 Hz, 3H); MS (FAB) *m/z* 530 (M+H).

4.1.4.7.

2-(3-Fluoro-4-methanesulfonylamino-phenyl)-N-(4-(trifluoromethyl)-2-(4-methylpiperidin-1-yl)phenyl)methyl)-propionamide (13).

Yield 58%, white solid, mp = 156-159 °C; ^{1}H NMR (300 MHz, $CDCl_3$) δ 7.48 (dd, *J* = 8.1, 8.1 Hz, 1H), 7.25-7.28 (m, 3H), 7.14 (dd, *J* = 8.1, 1.8 Hz, 1H), 7.07 (d, *J* = 8.1 Hz, 1H), 6.52 (*b*t, 1H), 4.51 (d, *J* = 5.1 Hz, 2H), 3.54 (q, *J* = 6.9 Hz, 1H), 3.01 (s, 3H), 2.96 (m, 2 H), 2.65 (m, 2H), 1.74 (m, 2H), 1.51(d, *J* = 6.9 Hz, 3H), 1.25 (m, 2H), 0.98 (d, *J* = 5.7 Hz, 3H); MS (FAB) *m/z* 516 (M+H).

4.1.4.8.

2-(3-Fluoro-4-methanesulfonylamino-phenyl)-N-(2-(4-ethyl-piperidin-1-yl)-4-trifluoro-methyl-benzyl)-propionamide (14).

Yield 59%, white solid, mp = 136 °C; ^{1}H NMR (300 MHz, $CDCl_3$) δ 7.51 (dd, *J* = 8.3, 8.3 Hz, 1H), 7.29 (s, 1H), 7.21-7.27 (m, 2H), 7.14 (m, 1H), 7.08 (d, *J* = 8.4 Hz, 1H), 6.48-6.59 (m, 2H), 4.46-4.60 (m, 2H), 3.53 (q, *J* = 6.9 Hz, 1H), 2.91-3.07 (m, 5H), 2.58-2.61 (m, 2H), 1.75-1.86 (m, 2H), 1.52 (d, *J* = 7.1 Hz, 3H), 1.10-1.37 (m, 5H), 0.93 (t, *J* = 7.0 Hz, 3H); MS (FAB) *m/z* 530 (M+H).

4.1.4.9.

2-(3-Fluoro-4-methanesulfonylamino-phenyl)-N-(2-(4,4-dimethyl-piperidin-1-yl)-4-trifluoromethyl-benzyl)-propionamide (15)

Yield 57%, white solid, mp = 85 °C; ^{1}H NMR (300 MHz, $CDCl_3$) δ 7.51 (dd, *J* = 8.3, 8.3 Hz, 1H), 7.32 (s, 1H), 7.21-7.30 (m, 2H), 7.14 (dd, *J* = 11.2,1.8 Hz, 1H), 7.08 (d, *J* = 8.6 Hz, 1H), 6.52 (bs, 2H), 4.45-4.60 (m, 2H), 3.54 (q, *J* = 7.1 Hz, 1H), 3.02 (s, 3H), 2.75-2.85 (m, 4H), 1.52 (d, *J* = 7.1 Hz, 3H), 1.42-1.50 (m, 4H), 1.00 (s, 6H); MS (FAB) *m/z* 530 (M+H).

4.1.4.10.

2-(3-Fluoro-4-methanesulfonylamino-phenyl)-N-[4-trifluoromethyl-2-(4-trifluoromethyl-piperidin-1-yl)-benzyl]-propionamide (16)

Yield 51%, white solid, mp = 85 °C; ^{1}H NMR (300 MHz, $CDCl_3$) δ 7.52 (dd, *J* = 8.2, 8.2 Hz, 1H), 7.22-7.32 (m, 3H), 7.12-7.19 (m, 1H), 7.09 (d, *J* = 8.3 Hz, 1H), 6.52 (bs, 1H), 6.12 (bt, 1H), 4.52 (d, *J* = 5.9 Hz, 2H), 3.56 (q, *J* = 7.1 Hz, 1H), 3.05-3.15 (m, 2H), 3.03 (bs, 3H), 2.62-2.77 (m, 2H), 2.08-2.24 (m, 1H), 1.93-2.02 (m, 2H), 1.61-1.74 (m, 2H), 1.54 (d, *J* = 7.1 Hz, 3H); MS (FAB) *m/z* 570 (M+H).

4.1.4.11.

2-(3-Fluoro-4-methanesulfonylamino-phenyl)-N-{2-[4-(4-fluoro-phenyl)-piperidin-1-yl]-4-trifluoromethyl-benzyl}-propionamide (17).

Yield 67%, white solid, mp = 165 °C; ^{1}H NMR (300 MHz, $CDCl_3$) δ 7.50 (dd, *J* = 8.3 Hz, 1H), 7.30-7.26 (m, 3H), 7.23-7.18 (m, 2H), 7.15 (dd, *J* = 11.8, 2.0 Hz, 1H), 7.08 (d, *J* = 10.0Hz, 1H, 7.03 (m, 2H), 6.46 (bs, 1H), 6.24 (bt, 1H), 4.56 (d, *J* = 5.7 Hz, 2H), 3.56 (q, *J* = 7.1 Hz, 1H), 3.09 (m, 2H), 3.00 (s, 3H), 2.83 (m, 2H), 2.64 (m, 1H), 1.94 (m, 2H), 1.78 (m, 2H), 1.54 (d, *J* = 6.9 Hz, 3H); MS (FAB) *m/z* 596 (M+H).

4.1.4.12.

2-(3-Fluoro-4-methanesulfonylamino-phenyl)-N-{2-(4-benzyl-piperidin-1-yl)-4-triflu-oromethyl-benzyl}-propionamide (18).

Yield 59%, white solid, mp = 93 °C; ^{1}H NMR (300 MHz, $CDCl_3$) δ 7.52 (dd, *J* = 8.2, 8.2 Hz, 1H), 7.27-7.35 (m, 3H), 7.20-7.26 (m, 2H), 7.11-7.19 (m, 4H), 7.08 (d, *J* = 8.2 Hz, 1H), 6.38-6.46 (m, 2H), 4.51 (d, *J* = 5.7 Hz, 2H), 3.52 (q, *J* = 7.1 Hz, 1H), 2.85-3.05 (m, 5H), 2.55-2.70 (m, 4H), 1.60-1.80 (m, 3H), 1.52 (d, *J* = 7.1 Hz, 3H), 1.21-1.38 (m, 2H); MS (FAB) *m/z* 592 (M+H).

4.1.4.13.

2-(3-Fluoro-4-(methylsulfonamido)phenyl)-N-(2-(4-(4-fluorobenzyl)piperidin-1-yl)-4-(trifluoromethyl)benzyl)propanamide (19).

Yield 65%, white solid, mp = 93 °C; ^{1}H NMR (300 MHz, $CDCl_3$) δ 7.52 (dd, *J* = 8.2, 8.2 Hz, 1H), 7.27-7.35 (m, 2H), 7.20-7.26 (m, 2H), 7.11-7.19 (m, 4H), 7.08 (d, *J* = 8.2 Hz, 1H), 6.38-6.46 (m, 2H), 4.51 (d, *J* = 5.7 Hz, 2H), 3.52 (q, *J* = 7.1 Hz, 1H), 2.85-3.05 (m, 5H), 2.55-2.70 (m, 4H), 1.60-1.80 (m, 3H), 1.52 (d, *J* = 7.1 Hz, 3H), 1.21-1.38 (m, 2H); MS (FAB) *m/z* 610 (M+H).

4.1.4.14.

2-(2-Fluoro-4-(methylsulfonamido)phenyl)-N-(2-(4-(4-fluorobenzyl)piperidin-1-yl)-4-(trifluoromethyl)benzyl)propanamide (20).

Yield 65%, white solid, mp = 93 °C; ^{1}H NMR (300 MHz, $CDCl_3$) δ 7.52 (dd, *J* = 8.2, 8.2 Hz, 1H), 7.27-7.35 (m, 2H), 7.20-7.26 (m, 2H), 7.11-7.19 (m, 4H), 7.08 (d, *J* = 8.2 Hz, 1H), 6.38-6.46 (m, 2H), 4.51 (d, *J* = 5.7 Hz, 2H), 3.52 (q, *J* = 7.1 Hz, 1H), 2.85-3.05 (m, 5H), 2.55-2.70 (m, 4H), 1.60-1.80 (m, 3H), 1.52 (d, *J* = 7.1 Hz, 3H), 1.21-1.38 (m, 2H); MS (FAB) *m/z* 610 (M+H).

4.1.4.15.

2-(3-Fluoro-4-methanesulfonylamino-phenyl)-N-[2-(4-cyclohexyl-piperazin-1-yl)-4-trifluoromethyl-benzyl]-propionamide (21).

Yield 54%, white solid, mp = 84.4 °C; ^{1}H NMR (300 MHz, $CDCl_3$) δ 7.52 (t, *J* = 8.2 Hz, 1H), 7.31 (s, 1H), 7.26-7.28 (m, 2H), 7.08-7.16 (m, 2H), 6.42 (bs, 1H), 4.52 (d, *J* = 5.9 Hz, 2H), 3.54 (q, *J* = 7.1 Hz, 1H), 3.0 (s, 3H), 2.88-2.95 (m, 4H), 2.67 (s, 3H), 1.81-1.90 (m, 3H), 1.64 (m, 2H), 1.52 (d, *J* = 7.0 Hz, 3H), 1.20-1.30 (m, 5H), 0.89-0.92 (m, 2H); MS (FAB) *m/z* 585 (M+H).

4.1.4.16.

2-(3-Fluoro-4-methanesulfonylamino-phenyl)-N-[2-(4-phenyl-piperazin-1-yl)-4-triflu-orometh yl-benzyl]-propionamide (22).

Yield 75%, white solid, mp = 100 °C; ^{1}H NMR (300MHz, $CDCl_3$) δ 7.46 (dd, *J* = 8.4, 8.4 Hz, 1H), 7.28-7.35 (m, 5H), 7.13 (m, 1H), 7.07 (d, *J* = 8.4 Hz, 1H), 6.89-6.99 (m, 3H), 6.32 (*b*t, 1H), 4.53-4.67 (m, 2H), 3.55 (q, *J* = 7.1 Hz, 1H), 3.20-3.28 (m, 4H), 3.00-3.08 (m, 4H), 2.98 (s, 3H), 1.51 (d, *J* = 6.9 Hz, 3H); MS (FAB) *m/z* 579 (M+H).

4.1.4.17. 2-(3-Fluoro-4-methanesulfonylamino-phenyl)-N-[2-(4-p-tolyl-piperazin-1-yl)-4-tri그 -uoromethyl-benzyl]-propionamide (23).

Yield 76%, white solid, mp = 165 °C; ^{1}H NMR (300 MHz, $CDCl_3$) δ 7.46 (dd, *J* = 8.2, 8.2 Hz, 1H), 7.34 (s, 1H), 7.33 (d, *J* = 7.5 Hz, 1H), 7.31 (d, *J* = 7.0 Hz, 1H), 7.13 (d, *J* = 8.1 Hz, 2H), 7.14 (dd, *J* = 11.2, 2.0 Hz, 1H), 7.08 (d, *J* = 10.0 Hz, 1H), 6.86 (d, *J* = 8.6 Hz, 2H), 6.35 (bt, 1H), 6.22 (bs, 1H), 4.57 (m, 2H), 3.54 (q, *J* = 7.0 Hz, 1H), 3.18-3.12 (m, 4H), 3.05-3.01 (m, 4H), 2.97 (s, 3H), 2.31 (s, 3H), 1.51 (d, *J* = 7.1 Hz, 3H); MS (FAB) *m/z* 593 (M+H).

4.1.4.18.

2-(3-Fluoro-4-methanesulfonylamino-phenyl)-N-[2-(4-m-tolyl-piperazin-1-yl)-4-trifl-uoromeththyl-benzyl]-propionamide (24).

Yield 68%, white solid, mp = 82-86 °C; ^{1}H NMR (300 MHz, $CDCl_3$) δ 7.46 (dd, *J* = 8.2 Hz, 1H), 7.36-7.26 (m, 3H), 7.21 (m, 1H), 7.13 (dd, *J* = 11.2, 2.0 Hz, 1H), 7.07 (d, *J* = 8.1, 8.1 Hz, 1H), 6.79-6.74 (m, 3H), 6.33 (*b*t, 1H), 6.25 (bs, 1H), 4.57 (m, 2H), 3.54 (q, *J* = 7.1 Hz, 1H), 3.24-3.18 (m, 4H), 3.08-3.01 (m, 4H), 2.97 (s, 3H), 2.36 (s, 3H), 1.51 (d, *J* = 7.1 Hz, 3H); MS (FAB) *m/z* 593 (M+H).

4.1.4.19.

2-(3-Fluoro-4-methanesulfonylamino-phenyl)-N-{4-trifluoromethyl-2-[4-(4-trifluoro-methyl-p

henyl)-piperazin-1-yl]-benzyl}-propionamide (25).

Yield 56%, white solid, mp = 210-213 °C; ^{1}H NMR (300 MHz, $CDCl_3$) δ 7.53 (d, *J* = 8.6 Hz, 2H), 7.50 (dd, *J* = 8.3, 8.3 Hz, 1H), 7.33 (s, 1H), 7.30 (d, *J* = 8.2 Hz, 2H), 7.14 (dd, *J* = 11.2, 2.0 Hz, 1H), 7.08 (d, *J* = 10.0 Hz, 1H), 6.97 (d, *J* = 8.9Hz, 2H), 6.23 (*b*t, 1H), 4.58 (d, *J* = 6.4 Hz, 2H), 3.54 (q, *J* = 7.1 Hz, 1H), 3.39-3.31 (m, 4H), 3.04-2.98 (m, 4H), 3.01 (s, 3H), 1.53 (d, *J* = 7.1 Hz, 3H); MS (FAB) *m/z* 647 (M+H).

4.1.4.20.

2-(3-Fluoro-4-methanesulfonylamino-phenyl)-N-{2-[4-(4-methoxy-phenyl)-piperazin-1-yl]-4-trifluoromethyl-benzyl}-propionamide (26).

Yield 71%, white solid, mp = 114 °C; ^{1}H NMR (300 MHz, $CDCl_3$) δ 7.47 (dd, *J* = 8.2, 8.2 Hz, 1H), 7.33 (d, *J* = 10.1 Hz, 2H), 7.29 (s, 1H), 7.13 (dd, *J* = 11.2, 2.0 Hz, 1H), 7.07 (d, *J* = 8.3 Hz, 1H), 6.98-6.85 (m, 4H), 6.35 (bs, 1H), 6.33 (bt, 1H), 4.59 (m, 2H), 3.80 (s, 3H), 3.54 (q, *J* = 7.1 Hz, 1H), 3.15-3.08 (m, 4H), 3.05-2.98 (m, 4H), 2.98 (s, 3H), 1.51 (d, *J* = 7.1 Hz, 3H); MS (FAB) *m/z* 609 (M+H).

4.1.4.21.

2-(3-Fluoro-4-methanesulfonylamino-phenyl)-N-(2-morpholin-4-yl-4-trifluoromethyl-benzyl)-propionamide (27).

Yield 80%, pale yellow solid, mp = 71-75 °C; ^{1}H NMR (300MHz, $CDCl_3$) δ 7.43 (t, *J* = 8.3 Hz, 1H), 7.16-7.24 (m, 3H), 7.09 (dd, *J* = 11.1, 2.0 Hz, 1H), 7.01 (dd, *J* = 7.8, 1.8 Hz, 1H), 6.70 (*b*s, 1H), 6.15 (bt, 1H), 4.47 (d, *J* = 5.4 Hz, 2H), 3.70 (t, *J* = 4.2 Hz, 4H), 3.50 (q, *J* = 7.2 Hz, 1H), 2.95 (s, 3H), 2.78 (t, *J* = 4.2 Hz, 4H), 1.45 (d, *J* = 7.2 Hz, 3H); MS (FAB) *m/z* 504 (M+H).

4.1.4.22.

2-(3-Fluoro-4-(methylsulfonamido)phenyl)-N-(2-(propyloxy)-4-(trifluoromethyl)ben-zyl)prop

anamide (28).

Yield 68%, white solid, mp = 98-105 °C; ^{1}H NMR (300 MHz, $CDCl_3$) δ 7.50 (t, *J* = 8.04 Hz, 1H), 7.26 (m, 1H), 7.16-7.02 (m, 4H), 6.43 (s, 1H), 5.90 (bs, 1H), 4.43 (m, 2H), 3.94 (m, 2H), 3.51 (q, *J* = 6.39 Hz, 1H), 3.00 (s, 3H), 1.78 (sext, *J* = 6.24 Hz, 2H), 1.50 (d, *J* = 7.14 Hz, 3H), 1.02 (t, *J* = 7.50 Hz, 3H); MS (FAB) *m/z* 477 (M+H).

4.1.4.23.

2-(3-Fluoro-4-(methylsulfonamido)phenyl)-N-(2-(butoxy)-4-(trifluoromethyl)benzyl)-propanamide (29).

Yield 47%, white solid, mp = 101 °C; ^{1}H NMR (300 MHz, $CDCl_3$) δ 7.50 (dd, *J* = 8.2, 8.2 Hz, 1H), 7.28 (m, 1H), 7.08-7.17 (m, 2H), 7.06 (d, *J* = 9.0 Hz, 1H), 7.02 (bs, 1H), 6.46 (bs, 1H), 5.93 (bt , 1H), 4.35-4.51 (m, 2H), 3.91-4.02 (m, 2H), 3.50 (q, *J* = 7.3 Hz, 1H), 3.02 (s, 3H), 1.67-1.80 (m, 2H), 1.39-1.53 (m, 5H), 0.98 (t , *J* = 7.3 Hz, 3H); MS (FAB) *m/z* 491 (M+H).

4.1.4.24.

2-(3-Fluoro-4-(methylsulfonamido)phenyl)-N-(2-(pentyloxy)-4(trifluoromethyl)benz-yl)propanamide (30).

Yield 57%, white solid, mp = 108 °C; ^{1}H NMR (300 MHz, $CDCl_3$) δ 7.49 (t, *J* = 8.43 Hz, 1H), 7.26 (m, 2H), 7.15-7.01 (m, 4H), 5.98 (bt, 1H), 4.43 (m, 2H), 3.97 (m, 2H), 3.50 (q, *J* = 6.96 Hz, 1H), 3.01 (s, 3H), 1.75 (m, 2H), 1.48 (t, *J* = 7.14 Hz, 3H), 1.42-1.39 (m, 4H), 0.94 (t, *J* = 6.96 Hz, 3H); MS (FAB) *m/z* 504 (M+H).

4.1.4.25.

2-(3-Fluoro-4-(methylsulfonamido)phenyl)-N-(2-(hexyloxy)-4(trifluoromethyl)benz-yl)propanamide (31).

Yield 50%, white solid, mp = 99-105 °C; ^{1}H NMR (300 MHz, $CDCl_3$) δ 7.48 (t, *J* = 8.79 Hz, 1H),

7.26 (m, 1H), 7.14-7.01 (m, 4H), 5.99 (bt, 1H), 4.43 (m, 2H), 3.98 (m, 2H), 3.50 (q, *J* = 7.14 Hz, 1H), 3.01 (s, 3H), 1.79-1.70 (m, 2H), 1.48 (t, *J* = 7.14 Hz, 3H), 1.44-1.28 (m, 6H), 0.94 (t, *J* = 6.78 Hz, 3H); MS (FAB) *m/z* 519 (M+H).

4.1.4.26.

2-(3-Fluoro-4-(methylsulfonamido)phenyl)-N-(2-(isobutyloxy)-4-(trifluoromethyl)be-nzyl)propanamide (32).

Yield 57%, white solid, mp = 105 °C; ^{1}H NMR (300 MHz, $CDCl_3$) δ 7.5 (t, *J* = 8.25 Hz, 1H), 7.26 (m, 1H), 7.16-7.01 (m, 4H), 6.42 (s, 1H), 5.88 (bs, 1H), 4.43 (m, 2H), 3.76 (dd, *J* = 2.4, 4.02 Hz, 2H), 3.50 (q, *J* = 6.96 Hz, 1H), 3.00 (s, 3H), 2.04 (pent, *J* = 6.78 Hz, 1H), 1.50 (d, *J* = 7.14 Hz, 3H), 1.02 (t, *J* = 6.78 Hz, 6H); MS (FAB) *m/z* 491 (M+H).

4.1.4.27.

2-(3-Fluoro-4-(methylsulfonamido)phenyl)-N-(2-(isopentyloxy)-4-(trifluoromethyl)-benzyl)propanamide (33).

Yield 60%, white solid, mp = 95-103 °C; ^{1}H NMR (300 MHz, $CDCl_3$) δ 7.50 (t, *J* = 8.07 Hz, 1H), 7.29 (m, 1H), 7.16-7.03 (m, 4H), 6.43 (bs, 1H), 5.90 (bt, 1H), 4.42 (m, 2H), 4.00 (m, 2H), 3.50 (q, *J* = 7.32 Hz, 1H), 3.02 (s, 3H), 1.79 (nonet, *J* = 6.78 Hz, 1H), 1.65 (q, *J* = 6.57 Hz, 2H), 1.50 (d, *J* = 7.14 Hz, 3H), 0.98 (t, *J* = 6.6 Hz, 6H); MS (FAB) *m/z* 505 (M+H).

4.1.4.28.

2-(3-Fluoro-4-(methylsulfonamido)phenyl)-N-(2-cyclopentyloxy)-4-(trifluoromethyl)-benzyl)propanamide (34).

Yield 41%, white solid, mp = 62 °C; ^{1}H NMR (300 MHz, $CDCl_3$) δ 7.51 (dd, *J* = 8.2, 8.2 Hz, 1H), 6.90-7.17 (m, 5H), 6.45 (bs, 1H), 5.90 (m, 1H), 4.80 (m, 1H), 4.31-4.47 (m, 2H), 3.49 (q, *J* = 7.1 Hz, 1H) 3.03 (s, 3H), 1.83-2.00 (m, 2H), 1.62-1.82 (m, 6H), 1.49 (d, *J* = 7.1 Hz, 3H); MS (FAB) *m/z*

503 (M+H).

4.1.4.29.

2-(3-Fluoro-4-(methylsulfonamido)phenyl)-N-(2-cyclohexyloxy)-4-(trifluoromethyl)-benzyl)propanamide (35).

Yield 63%, white solid, mp = 103 °C; ^{1}H NMR (300 MHz, $CDCl_3$) δ 7.51 (dd, *J* = 8.4, 8.4 Hz, 1H), 7.30 (m, 1H), 7.09-7.10 (m, 2H), 7.06 (d, *J* = 8.3 Hz, 1H), 7.02 (bs, 1H), 6.47 (bs, 1H), 5.53 (m, 1H), 4.27-4.50 (m, 2H), 3.50 (q, *J* = 7.0 Hz, 1H), 3.02 (s, 3H), 1.84-1.96 (m, 2H), 1.64-1.78 (m, 2H), 1.25-1.63 (m, 9H); MS (FAB) *m/z* 517 (M+H).

4.1.4.30.

2-(3-Fluoro-4-(methylsulfonamido)phenyl)-N-(2-benzyloxy)-4-(trifluoromethyl)ben-zyl)propanamide (36).

Yield 59%, white solid, mp = 89-91 °C; ^{1}H NMR (300 MHz, $CDCl_3$) δ 7.44 (dd, *J* = 8.4, 8.4 Hz, 1H), 7.41-7.34 (m, 5H), 7.33 (d, *J* = 8.6 Hz, 1H), 7.19 (d, *J* = 7.9 Hz, 1H), 7.14 (s, 1H), 7.05 (dd, *J* = 11.3, 2.0 Hz, 1H), 6.95 (d, *J* = 6.4 Hz, 1H), 6.41 (bs, 1H), 5.94 (bt, 1H), 5.08 (s, 2H), 4.46 (m, 2H), 3.41 (q, *J* = 7.0 Hz, 1H), 2.99 (s, 3H), 1.43 (d, *J* = 7.1 Hz, 3H); MS (FAB) *m/z* 525 (M+H).

4.1.4.31.

2-(3-Fluoro-4-(methylsulfonamido)phenyl)-N-(2-((4-fluorobenzyl)oxy)-4-(trifluorom-ethyl)benzyl)propanamide (37).

Yield 71%, white solid, mp = 86-90 °C; ^{1}H NMR (300 MHz, $CDCl_3$) δ 7.48 (t, *J* = 8.07 Hz, 1H), 7.36-7.21 (m, 4H), 7.12-7.03 (m, 4H), 6.98 (m, 1H), 6.43 (s, 1H), 4.45 (bs, 1H), 3.44 (q, *J* = 7.14 Hz, 1H), 3.00 (s, 3H), 1.45 (d, *J* = 7.14 Hz, 3H); MS (FAB) *m/z* 543 (M+H).

4.1.4.32.

2-(3-Fluoro-4-(methylsulfonamido)phenyl)-N-(2-(butylthio)-4(trifluoromethyl)benz-yl)propan amide (38).

Yield 65%, white solid, mp = 95 °C; ^{1}H NMR (300 MHz, $CDCl_3$) δ 7.53-7.37 (m, 2H), 7.34-7.31 (m, 2H), 7.15-7.06 (m, 2H), 6.59 (bs, 1H), 5.99 (bt, 1H), 4.49 (m, 2H), 3.50 (q, *J* = 7.32 Hz, 1H), 3.02 (s, 3H), 2.93 (t, *J* = 7.32 Hz, 2H), 1.67-1.58(m, 2H), 1.50-1.39 (m, 5H), 0.94 (t, *J* = 7.14 Hz, 3H); MS (FAB) *m/z* 507 (M+H).

4.1.4.33.

2-(3-Fluoro-4-(methylsulfonamido)phenyl)-N-(2-(pentylthio)-4-(trifluoromethyl)ben-zyl)prop anamide (39).

Yield 72%, white solid, mp = 95 °C; ^{1}H NMR (300 MHz, $CDCl_3$) δ 7.53-7.47 (m, 2H), 7.73-7.31 (m, 2H), 7.13 (dd, *J* = 11.3 Hz, 2.9 Hz, 1H), 7.07 (d, *J* = 8.61 Hz, 1H), 6.66 (bs, 1H), 6.04 (t, *J* = 5.7 Hz, 1H), 4.48 (m, 2H), 3.55 (q, *J* = 6.96 Hz, 1H), 3.01 (s, 3H), 2.92 (t, *J* = 7.32 Hz, 2H), 1.69-1.60 (m, 2H), 1.49 (d, *J* = 7.14 Hz, 3H), 1.44-1.30 (m, 4H), 0.90 (d, *J* = 6.96 Hz, 3H); MS (FAB) *m/z* 521 (M+H).

4.1.4.34.

2-(3-Fluoro-4-(methylsulfonamido)phenyl)-N-(2-(hexylthio)-4(trifluoromethyl)benz-yl)propan amide (40).

Yield 81%, white solid, mp = 92 °C; ^{1}H NMR (300 MHz, $CDCl_3$) δ 7.51 (t, *J* = 8.25 Hz, 1H), 7.47 (s, 1H), 7.37-7.31 (m, 2H), 7.15-7.06 (m, 2H), 6.42 (bs, 1H), 5.92 (bt, 1H), 4.49 (t, *J* = 5.49 Hz, 2H), 3.51 (q, *J* = 7.32 Hz, 1H), 3.02 (s, 3H), 2.92 (t, *J* = 7.32 Hz, 2H), 1.64(m, 2H), 1.51(d, *J* = 7.14 Hz, 3H), 1.45-1.25(m, 6H), 0.89 (t, *J* = 6.78 Hz, 3H); MS (FAB) *m/z* 535 (M+H).

4.1.4.35.

2-(3-Fluoro-4-(methylsulfonamido)phenyl)-N-(2-(isopentylthio)-4-(trifluoromethyl)-benzyl)pr

opanamide (41).

Yield 75%, white solid, mp = 95 °C; ^{1}H NMR (300 MHz, $CDCl_3$) δ 7.51 (t, *J* = 8.25 Hz, 1H), 7.47 (s, 1H), 7.35 (m, 2H), 7.16-7.06 (m, 2H), 6.44 (bs, 1H), 5.91 (bt, 1H), 4.48 (m, 2H), 3.54 (q, *J* = 6.51 Hz, 1H), 2.29 (s, 3H), 2.93 (t, *J* = 7.5 Hz, 2H), 1.72 (nonet, *J* = 6.78 Hz, 1H), 1.55 (m, 2H), 1.50 (d, *J* = 7.14 Hz, 3H), 0.93 (d, *J* = 6.6 Hz, 6H); MS (FAB) *m/z* 521 (M+H).

4.1.4.36.

2-(3-Fluoro-4-(methylsulfonamido)phenyl)-N-(2-((3-hydroxypropyl)thio)-4-(trifluoro-methyl) benzyl)propanamide (42).

Yield 67%, yellow oil, mp = 105 °C; ^{1}H NMR (300 MHz, $CDCl_3$) δ 7.52-7.47 (m, 2H), 7.39-7.32 (m, 2H), 7.13-7.06 (m, 2H), 6.03 (m, 1H), 4.49 (d, 2H), 3.76 (t, *J* = 6.00 Hz, 2H), 3.54 (q, *J* = 6.96 Hz, 1H), 3.06-3.01 (m, 5H), 1.86 (m, 2H), 1.49 (d, *J* = 7.14 Hz, 3H); MS (FAB) *m/z* 509 (M+H).

4.1.4.37.

2-(3-Fluoro-4-(methylsulfonamido)phenyl)-N-(2-cyclopentylthio-4-(trifluoromethyl)-benzyl)pr opanamide (43).

Yield 80%, pale yellow oil, mp = 90 °C; ^{1}H NMR (300 MHz, $CDCl_3$) δ 7.54-7.48 (m, 2H), 7.35 (m, 2H), 7.15-7.06 (m, 2H), 6.40 (m, 1H), 5.90 (bt, 1H), 4.49 (d, *J* = 6.21 Hz, 2H), 3.63-3.49 (m, 2H), 3.02 (s, 3H), 2.17 (m, 2H), 1.78 (m, 2H), 1.65-1.48 (m, 4H), 1.50 (d, *J* = 7.14 Hz 3H); MS (FAB) *m/z* 519 (M+H).

4.1.4.38.

2-(3-Fluoro-4-(methylsulfonamido)phenyl)-N-(2-(cyclohexylthio)-4(trifluoromethyl)-benzyl)pr opanamide (44).

Yield 78%, white solid, mp = 101 °C; ^{1}H NMR (300 MHz, $CDCl_3$) δ 7.59 (s, 1H), 7.51 (t, *J* = 8.43 Hz, 1H), 7.38 (m, 2H), 7.13-7.06 (m, 2H), 6.48 (bs, 1H), 5.91 (bt, 1H), 4.54 (d, *J* = 5.85 Hz, 2H),

3.52 (q, *J* = 7.32 Hz, 1H), 3.13 (m, 1H), 3.02 (s, 3H), 1.91 (m, 2H), 1.76 (m, 2H), 1.58 (m, 2H), 1.49 (d, *J* = 7.14 Hz, 3H), 1.34-1.31 (m, 4H); MS (FAB) *m/z* 533 (M+H).

4.1.4.39.

2-(3-Fluoro-4-(methylsulfonamido)phenyl)-N-(2-(benzylthio)-4(trifluoromethyl)ben-zyl)propanamide (45).

Yield 81%, white solid, mp = 102 °C; ^{1}H NMR (300 MHz, $CDCl_3$) δ 7.55 (s, 1H), 7.50 (t, *J* = 8.22 Hz, 1H), 7.40-7.25 (m, 5H), 7.15-7.03 (m, 4H), 6.45 (bs, 1H), 5.68 (bt, 1H), 4.39 (m, 2H), 4.06 (s, 2H), 3.46 (q, *J* = 7.14 Hz, 1H), 3.00 (s, 3H), 1.47 (d, *J* = 7.14 Hz, 3H); MS (FAB) *m/z* 541 (M+H).

4.1.4.40.

2-(3-Fluoro-4-(methylsulfonamido)phenyl)-N-(2-cyclopentylthio-4-(trifluoromethyl)-benzyl)propanamide (46).

Yield 51%, white solid, mp = 101 °C; ^{1}H NMR (300 MHz, CD_3OD) δ 7.54-7.48 (m, 2H), 7.41 (d, *J* = 7.0 Hz, 1H), 7.33 (d, *J* = 8.0 Hz, 1H), 7.25 (m, 2H), 7.05-7.14 (m, 4H), 4.41 (m, 2H), 4.04 (s, 2H), 3.45 (q, *J* = 7.0 Hz, 1H), 3.01 (s, 3H), 1.47 (d, *J* = 7.14 Hz, 3H); MS (FAB) *m/z* 575 (M+H).

4.1.4.41.

2-(3-Fluoro-4-(methylsulfonamido)phenyl)-N-(2-(2-chlorobenzylthio)-4-(trifluorom-ethyl)benzyl)propanamide (47).

Yield 60%, white solid, mp = 101 °C; ^{1}H NMR (300 MHz, $CDCl_3$) δ 7.53-7.35 (m, 4H), 7.24-7.03 (m, 6H), 6.45 (bs, 1H), 5.86 (bt, 1H), 4.41 (m, 2H), 4.16 (s, 2H), 3.47 (q, *J* = 7.14 Hz, 1H), 3.01 (s, 3H), 1.47 (d, *J* = 7.14 Hz, 3H); MS (FAB) *m/z* 575 (M+H).

4.1.4.42.

2-(3-Fluoro-4-(methylsulfonamido)phenyl)-N-(2-((4-methoxybenzyl)thio)-4-(trifluo-romethyl)

benzyl)propanamide (48).

Yield 69%, white solid, mp = 103 °C; ^{1}H NMR (300 MHz, DMSO) δ 9.61 (bs, 1H), 8.55 (t, *J* = 5.67 Hz, 1H), 7.57 (s, 1H), 7.45 (d, *J* = 7.68 Hz, 1H), 7.35-7.13 (m, 6H), 6.87 (d, *J* = 8.61 Hz, 2H), 4.28 (m, 4H), 3.71 (s, 3H), 3.34 (bs, 1H), 3.00 (s, 3H), 1.37 (d, *J* = 6.96 Hz, 3H); MS (FAB) *m/z* 571 (M+H).

4.1.4.43.

2-(3-Fluoro-4-(methylsulfonamido)phenyl)-N-(2-cyclopentylthio-4-(trifluoromethyl)-benzyl)propanamide (49).

Yield 91%, white solid, mp = 98 °C; ^{1}H NMR (300 MHz, CDCl3) δ 7.33-7.57 (m, 6H), 7.04-7.13 (m, 2H), 6.26 (bs, 1H), 6.01 (m, 1H), 4.42 (m, 2H), 4.06 (s, 2H), 3.49 (q, *J* = 7.1 Hz, 1H), 3.03 (s, 3H), 1.49 (d, *J* = 7.1 Hz, 3H); MS (FAB) *m/z* 531 (M+H).

4.1.4.44.

2-(3-Fluoro-4-methanesulfonylamino-phenyl)-N-(2-fluoro-4-trifluoromethyl-benzyl)-propioamide (50).

Yield 49%, white solid, mp = 138 °C; ^{1}H NMR (300 MHz, $CDCl_3$) δ 7.50 (dd, *J* = 8.0, 8.0 Hz, 1H), 7.41-7.26 (m, 3H), 7.13 (dd, *J* = 11.0, 2.0 Hz, 1H), 7.07 (bd, 1H), 6.60 (bs, 1H), 6.00 (bt, 1H), 4.48 (m, 2H), 3.03 (s, 3H), 1.49 (d, *J* = 7.1 Hz, 3H); MS (FAB) *m/z* 437 (M+H).

4.1.4.45.

2-(3-Fluoro-4-methanesulfonylamino-phenyl)-N-(2-chloro-4-trifluoromethyl-benzyl)-propionamide (51).

Yield 65%, white solid, mp 90 °C; ^{1}H NMR (300MHz, $CDCl_3$) δ 7.52 (s, 1 H), 7.30-7.45(m, 3 H), 6.98-7.08(m, 2H), 6.65 (bs, 1H), 6.01 (bt, 1H), 4.40 (d, *J* = 5.7 Hz, 2H), 3.50 (q, *J* = 7.2 Hz, 1H), 2.95 (s, 3H), 1.43 (d, *J* = 7.2 Hz, 3H); MS (FAB) *m/z* 453 (M+H).

4.1.4.46.

2-(3-Fluoro-4-methanesulfonylamino-phenyl)-N-(2-nitro-4-trifluoromethyl-benzyl)-propiona mide (52).

Yield 27%, white solid, mp = 81 °C; ^{1}H NMR (300MHz, $CDCl_3$) δ 8.29(s, 1 H), 7.86 (d, *J* = 8.0 Hz, 1H), 7.76 (d, *J* = 8.0 Hz, 1H), 7.09-7.03 (m, 2H), 6.54 (bs, 1H), 6.27 (bt, 1H), 4.67 (d, *J* = 6.2 Hz, 2H), 3.53 (q, *J* = 7.0 Hz, 1H), 3.05(s, 3H), 1.47 (d, *J* = 7.1 Hz, 3H); MS (FAB) m/z 464 (M+H).

4.1.4.47.

2-(3-Fluoro-4-(methylsulfonamido)phenyl)-N-(2-hexyl-4-(trifluoromethyl)benzyl)pro-panami de (53).

Yield 80%, pale yellow oil, mp = 85 °C; ^{1}H NMR (300 MHz, $CDCl_3$) δ 7.55 (t, *J* = 8.22 Hz, 1H), 7.52 (m, 1H), 7.22-7.09 (m, 3H), 6.47 (s, 1H), 5.59 (bs, 1H), 4.45 (m, 2H), 3.55 (q, *J* = 7.14 Hz, 1H), 3.02 (s, 3H), 2.06 (t, *J* = 8.25 Hz, 2H), 1.54 (m, 5H), 1.33 (m, 4H), 0.89 (m, 3H); MS (FAB) *m/z* 489 (M+H).

4.1.4.48.

2-(3-Fluoro-4-(methylsulfonamido)phenyl)-N-(2-(cyclohexyl)-4-(trifluoromethyl)ben-zyl)prop anamide (54).

Yield 80%, pale yellow oil, mp = 90 °C; ^{1}H NMR (300 MHz, $CDCl_3$) δ 7.54-7.48 (m, 2H), 7.36 (m, 1H), 7.22 (d, *J* = 7.80 Hz, 1H), 7.16 (dd, *J* = 8.1, 1.8 Hz, 1H), 7.08 (d, *J* = 8.40 Hz, 1H), 6.53 (s, 1H), 5.57 (bs, 1H), 4.50 (m, 2H), 3.52 (q, *J* = 6.90 Hz, 1H), 3.01 (s, 3H), 2.65 (m, 1H), 1.82-1.23 (m, 13H); MS (FAB) *m/z* 501 (M+H).

4.1.4.49.

2-(3-Fluoro-4-methanesulfonylamino-phenyl)-N-(4'-methoxy-5-trifluoromethyl-biph-enyl-2-yl

methyl)-propionamide (55).

Yield 98%, white solid, mp = 133 °C; ^{1}H NMR (300 MHz, $CDCl_3$) δ 7.46-7.54 (m, 3H), 7.39 (d, *J* = 8.0 Hz, 1H), 7.14 (dd, *J* = 6.4, 2.0 Hz, 2H), 7.05 (dd, *J* = 11.0, 1.8 Hz, 1H), 6.99 (d, *J* = 8.3 Hz, 1H), 6.93 (dd, *J* = 6.8, 2.2 Hz, 2H), 5.46 (bt, 1H), 4.43 (t, *J* = 3.7 Hz, 2H), 3.86 (s, 3H), 3.43 (q, *J* = 7.5 Hz, 1H), 3.02 (s, 3H), 1.44 (d, *J* = 7.0 Hz, 3H); MS (FAB) *m/z* 525(M+H).

4.1.4.50.

2-(3-Fluoro-4-methanesulfonylamino-phenyl)-N-(4'-tert-butyl-5-trifluoromethyl-bip-henyl-2-ylmethyl)-propionamide (56).

Yield 93%, white solid, mp = 91 °C; ^{1}H NMR (300 MHz, $CDCl_3$) δ 7.28-7.55 (m, 6H), 7.16 (d, *J* = 7.4 Hz, 2H), 7.07 (dd, *J* = 11.2, 1.8 Hz, 1H), 6.97~7.02 (m, 1H), 5.51 (bt, 1H), 4.41-4.51 (m, 2H), 3.43 (q, *J* = 7.1 Hz, 1H), 3.0 (s, 3H), 1.44 (d, *J* = 7.1 Hz, 3H), 1.36 (s, 9 H); MS (FAB) *m/z* 551 (M+H).

4.1.4.51.

2-(3-Fluoro-4-methanesulfonylamino-phenyl)-N-(3'-fluoro-5-trifluoromethyl-biphen-yl-2-ylmethyl)-propionamide (57).

Yield 68%, white solid, mp = 155 °C; ^{1}H NMR (300 MHz, $CDCl_3$) δ 7.38-7.59 (m, 5H), 7.00-7.09 (m, 4H), 6.93 (d, *J* = 10.4 Hz, 1H) 4.39 (m, 2H), 3.45 (q, *J* = 7.3 Hz, 1H), 3.03 (s, 3H), 1.46 (d, *J* = 7.1 Hz, 3H); MS (FAB) *m/z* 513 (M+H).

4.1.4.52.

2-(3-Fluoro-4-methanesulfonylamino-phenyl)-N-(3'-chloro-5-trifluoromethyl-biphen-yl-2-ylmethyl)-propionamide (58).

Yield 66%, white solid, mp = 146 °C; ^{1}H NMR (300 MHz, $CDCl_3$) δ 7.58-7.32 (m, 6H), 7.23 (m, 1H), 7.14-7.00 (m, 3H), 5.61 (bt, 1H), 4.39 (t, *J* = 5.5 Hz, 2H), 3.46 (q, *J* = 7.1 Hz, 1H), 3.0 (s, 3H),

1.45 (d, *J* = 7.1 Hz, 3H); MS (FAB) *m/z* 528 (M+H).

4.1.4.53.

2-(3-Fluoro-4-methanesulfonylamino-phenyl)-N-(3'-chloro-4'-fluoro-5-trifluorometh-yl-biphenyl-2-ylmethyl)-propionamide (59).

Yield 68%, white solid, mp = 164 °C; ^{1}H NMR (300 MHz, $CDCl_3$) δ 7.49-7.59 (m, 2H), 7.37-7.44 (m, 2H), 7.02-7.22 (m, 5H), 5.54 (bt, 1H), 4.38 (d, *J* = 6.0Hz, 2H), 3.49 (q, *J* = 7.0 Hz, 1H), 3.04 (s, 3H), 1.47 (d, *J* = 7.1 Hz, 3H); MS (FAB) *m/z* 548 (M+H).

4.1.4.54.

2-(3-Fluoro-4-methanesulfonylamino-phenyl)-N-(3',4'-dimethoxy-5-trifluoromethyl-biphenyl-2-ylmethyl)-propionamide (60).

Yield 43%, white solid, mp = 114 °C; ^{1}H NMR (300 MHz, $CDCl_3$) δ 7.43-7.53 (m, 3H), 7.38 (d, *J* = 8.1 Hz, 1H), 7.07 (dd, *J* = 11.3, 2.0 Hz, 1H), 7.0 (d, *J* = 8.2 Hz, 1H), 6.90 (d, *J* = 8.2 Hz, 1H), 6.74-6.77 (m, 2H), 5.72 (bs, 1H), 4.44 (m, 2H), 3.92 (s, 3H), 3.86 (s, 3), 3.46 (q, *J* = 7.1 Hz, 1H), 3.01 (s, 3H), 1.44 (d, *J* = 7.1 Hz, 3H); MS (FAB) *m/z* 555 (M+H).

4.1.4.55.

2-(3-Fluoro-4-methanesulfonylamino-phenyl)-N-(3',5'-dimethoxy-5-trifluoromethyl-biphenyl-2-ylmethyl)-propionamide (61).

Yield 34%, white solid, mp = 85 °C; ^{1}H NMR (300 MHz, $CDCl_3$) δ 7.40-7.56 (m, 4H), 6.98-7.08 (m, 2H), 6.48 (t, *J* = 2.4 Hz, 1H), 6.35 (d, *J* = 2.2 Hz, 2H), 5.56 (bt, 1H), 4.43 (t, *J* = 5.5 Hz, 2H), 3.81 (s, 6H), 3.43 (q, *J* = 7.2 Hz, 1H), 3.02 (s, 3H), 1.44 (d, *J* = 7.1 Hz, 3H); MS (FAB) *m/z* 555 (M+H).

4.1.4.56.

2-(3-Fluoro-4-methanesulfonylamino-phenyl)-N-(2-pyridin-3-yl-4-trifluoromethylbe-nzyl)-propionamide (62).

Yield 26%, white solid, mp = 84 °C; ^{1}H NMR (300 MHz, $CDCl_3$) δ 8.62 (dd, *J* = 4.8, 1.7 Hz, 1H), 8.50 (d, *J* = 2.2 Hz, 1H), 7.59-7.66 (m, 2H), 7.44-7.49 (m, 3H), 7.38 (m, 1H), 7.01-7.11 (m, 2H), 6.05 (bt, 1H), 4.36 (m, 2H), 3.51 (m, 1H), 3.0 (s, 3H), 1.45 (d, *J* = 7.1 Hz, 3H); MS (FAB) *m/z* 496 (M+H).

4.2. Molecular modeling

The 3D structure of the **44*S*** was generated with Concord and energy minimized with an MMFF94s force field and MMFF94 charge until the rms of the Powell gradient was 0.05 kcal $mol^{-1}A^{-1}$ in SYBYL-X 2.0 (Tripos Int., St. Louis, MO, USA). The flexible docking study on our *h*TRPV1 model was performed using GOLD v.5.2 (Cambridge Crystallographic Data Centre, Cambridge, UK), which uses a genetic algorithm (GA) and allows for full ligand flexibility and partial protein flexibility. The binding site was defined as 8 Å around the capsaicin complexed in the *h*TRPV1 model. The side chains of the nine residues which are important for ligand binding, (i.e., Tyr511, Ser512, Met514, Leu515, Leu518, Phe543, Leu547, Thr550, and Asn551) were allowed to be flexible with 'crystal mode' in GOLD. **44*S*** was docked with the GoldScore scoring function, and the other parameters remained as default. All the computation calculations were undertaken on an Intel® Xeon™ Quad-core 2.5 GHz workstation with Linux Cent OS release 5.5.

Acknowledgments

This research was supported by research grants from Grünenthal in Germany, grants from the Korea Science and Engineering Foundation (KOSEF) (NRF-2007-0057057) and the National Leading Research Lab (NLRL) program (2011-0028885) in South Korea, and in part by the Intramural Research Program of the NIH, Center for Cancer Research, NCI (Project Z1A BC 005270) in the USA.

References and Notes

1. Szallasi, A.; Blumberg, P. M. *Pharmacol. Rev*. **1999**, 51, 159.

2. Tominaga, M.; Caterina, M. J.; Malmberg, A. B.; Rosen, T. A.; Gilbert, H.; Skinner, K.; Raumann, B. E.; Basbaum, A. I.; Julius, D. *Neuron* **1998**, 21, 531.

3. Szallasi, A. *Am. J. Clin. Pathol*. **2002**, 118, 110.

4. (a) Walpole, C.S.; Wrigglesworth, R.; Bevan, S.; Campbell, E.A.; Dray, A.; James, I.F.; Perins, M.N.; Reid, D.J.; Winter, J. *J. Med. Chem*. **1993,** 36, 2362. (b) Walpole, C.S.; Wrigglesworth, R.; Bevan, S.; Campbell, E.A.; Dray, A.; James, I.F.; Masdin, K.J.; Perkins, M.N.; Winter, J. *J. Med. Chem*. **1993**, 36, 2373. (c) Walpole, C.S.; Wrigglesworth, R., Bevan,S., Campbell, E.A., Dray, A., James, I.F., Masdin, K.J., Perkins, M.N., Winter, J. *J. Med. Chem*. **1993**, 36, 2381.

5. Appendino, G.; Szallasi, A. *Life Sci*. **1997**, 60, 681.

6. (a) Kym, P. R.; Kort, M. E.; Hutchins, C. W. *Biochem. Pharmacol*. **2009**, 78, 211. (b) Wong, G. Y.; Gavva, N. R. *Brain Res. Rev*. **2009**, 60, 267. (c) Gunthorpe, M. J.; Chizh, B. A. *Drug Disc. Today* **2009**, 14, 56. (d) Lazar, J.; Gharat, L.; Khairathkar-Joshi, N.; Blumberg, P. M.; Szallasi, A. *Exp. Opin. Drug Discov.* **2009**, 4, 159. (e) Voight, E. A.; Kort, M. E. *Exp. Opin. Ther. Pat*. **2010**, 20, 1. (f) Szolcsányi, J.; Sándor, Z. *Trend Pharmacol. Sci*. **2012**, 33, 646. (g) Szallasi, A.; Sheta, M. *Exp. Opin. Investig. Drug* **2012**, 21, 1351. (h) De Petrocellis L.; Moriello A. S. *Recent Patents on CNS Drug Discovery* **2013**, 8, 180-204. (i) Lee, Y.; Hong, S.; Cui, M.; Sharma, P. K. Lee, J.; Choi, S. *Exp. Opin. Ther. Pat*. **2015**, 25, 291.

7. Wang, Y.; Toth, A.; Tran, R.; Szabo, T.; Wleter, J.D.; Blumberg, P.M.; Lee, J.; Kang, S.U.; Lim, J.O.; Lee, J. *Mol. Pharmacol*. **2003**, 64, 325.

8. Garami, A.; Shimansky, Y.P.; Pakai, E.; Oliveira, D.L.; Gavva, N.R.; Romanovsky, A.A. *J. Neurosci*. **2010**, 30, 1435.

9. Kim, M. S.; Ryu, H.; Kang, D. W.; Cho, S-H.; Seo, S.; Park, Y. S.; Kim, M-Y.; Kwak, E. J.; Kim, Y. S.; Bhondwe, R. S.; Kim, H. S.; Park, S-g. Son, K.; Choi, S.; DeAndrea-Lazarus, I.; Pearce, L. V.; Blumberg, P. M.; Frank, R.; Bahrenberg, G.; Stockhausen, H.; Kögel, B. Y.; Schiene, K.; Christoph,

T.; Lee, J. *J. Med. Chem.* **2012**, 55, 8392.

10. Thorat, S. A.; Kang, D. W.; Ryu, H.; Kim, M. S.; Kim, H. S.; Ann, J.; Ha, T-H.; Kim, S. E.; Son, K.; Choi, S.; Blumberg, P. M.; Frank, R.; Bahrenberg, G.; Schiene, K.; Christoph, T.; Lee, J. *Eur. J. Med. Chem.* **2013**, 64, 589.

11. Ha, T-H; Ryu, H.; Kim, S-E.; Kim, H. S.; Ann, J.; Tran, P-T.; Hoang, V-H.; Son, K.; Cui, M.; Choi, S.; Blumberg, P. M.; Frank, R.; Bahrenberg, G.; Schiene, K.; Christoph, T.; Frormann, S.; Lee, J. *Bioorg. Med. Chem.* **2013**, 21, 6657.

12. Ryu, H.; Seo, S.; Cho, S-H.; Kim, H. S.; Jung, A.; Kang, D. W.; Son, K.; Cui, M.; Hong, S-h.; Sharma, P. K.; Choi, S.; Blumberg, P. M.; Frank-Foltyn, R.; Bahrenberg, G.; Stockhausen, H.; Schiene, K.; Christoph, T,; Frormann, S.; Lee, J. *Bioorg. Med. Chem. Lett.* **2014**, 24, 4039.

13. Ryu, H.; Seo, S.; Cho, S-H.; Kim, M. S.; Kim, M-Y.; Kim, H. S.; Ann, J.; Tran, P-T.; Hoang, V-H,; Byun, J.; Cui, M.; Son, K.; Sharma, P. K.; Choi, S.; Blumberg, P. M.; Frank-Foltyn, R.; Bahrenberg, G.; Koegel, B-Y.; Christoph, T.; Frormann, S.; Lee, J. *Bioorg. Med. Chem. Lett.* **2014**, 24, 4044.

14. Ryu, H.; Seo, S.; Lee, J-Y.; Ha, T-H.; Lee, S.; Jung, A.; Ann, J.; Kim, S-E.; Yoon, S.; Hong, M.; Blumberg, P. M.; Frank-Foltyn, R.; Bahrenberg, G.; Schiene, K.; Stockhausen, H.; Christoph, T.; Frormann, S.; Lee, J. *Eur. J. Med. Chem.* **2015**, 93, 101.

15. Lee, J. H.; Lee, Y.; Ryu, H.; Kang, D. W.; Lee, J.; Lazar, J.; Pearce, L. V; Pavlyukovets, V. A.; Blumberg, P. M.; Choi, S. *J. Comput. Aided Mol. Des.* **2011**, 25, 317.

Legends

Figure 1. 4-(Trifluoromethyl)benzyl C-region TRPV1 antagonists

Scheme 1. General synthesis of 2-(3-fluoro-4-(methylsulfonamido)phenyl) propanamide analogues

Table 1. *In vitro h*TRPV1 antagonistic activities for 2-amino derivatives

Table 2. *In vitro h*TRPV1 antagonistic activities for 2-oxy derivatives

Table 3. *In vitro h*TRPV1 antagonistic activities for 2-thio derivatives

Table 4. *In vitro h*TRPV1 antagonistic activities for 2-halo, alkyl and aryl derivatives

Table 5. Comparison of *in vitro h*TRPV1 antagonistic activities for representative, corresponding antagonists from the pyridine and phenyl C-region series

Table 6. *In vitro h*TRPV1 antagonistic activities of **43** and **44*S*** for multiple activators.

Table 7. Inhibition of capsaicin-induced hypothermia after oral administration in the mouse. Data, n = 10, mean ± SEM, * $p<0.05$ vs. vehicle.

Figure 2. Analgesic activity of compounds **43**, **44*S*** on CCI-induced cold allodynia (Bennett model) after oral administration in the mouse. Data, n = 10, mean ± SEM, * $p<0.05$ vs. vehicle. MPE, maximal possible effect.

Figure 3. Docking result of **44*S*** in the *h*TRPV1 model.

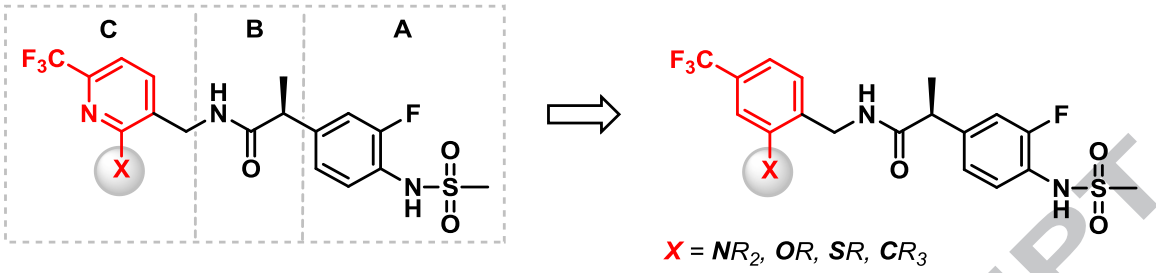

Figure 1. 4-(Trifluoromethyl)benzyl C-region TRPV1 antagonists

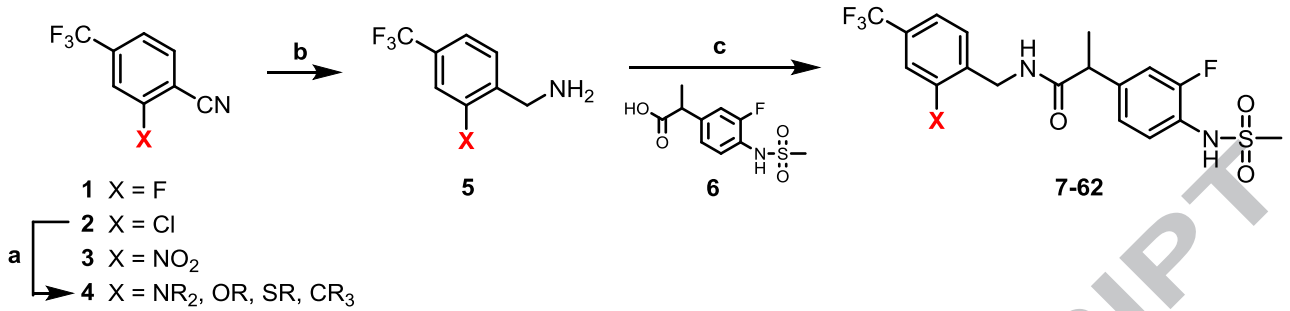

Scheme 1. General synthesis of 2-(3-fluoro-4-(methylsulfonamido)phenyl) propanamide analogues
Reagents and conditions: (a) [Method A] NR_2, DBU, 1,4-dioxane, 50 ºC, 12 h for **7-26**; [Method B] neat NR_2, DMF, 120 ºC, 6 h for **27**; [Method C] ROH, KO^tBu, Toluene/DMBU, 70 ºC, 5 h for **28-35**; [Method D] neat ROH, DBU, 80 ºC, 3 h for **36, 37**; [Method E] RSH, K_2CO_3, 18-Crown-6, CH_3CN, reflux**,** 12 h for **38-49**; [Method F] R-$B(OH)_2$, $Pd(PPh_3)_4$, dppf, toluene/1,4-dioxane/2N Na_2CO_3, reflux, 12 h for **53-62**; (b) [Method G] H_2, 10% Pd-C, c-HCl, MeOH, 40 ºC, 8 h for **17, 27, 54**; [Method H] 2M $BH_3{\cdot}SMe_2$ in THF, reflux, 12 h for **7-16, 18-26**, **28-53, 55-62**; (c) EDC, HOBt, DMF, room temperature, 12 h.

Table 1. *In vitro h*TRPV1 antagonistic activities for 2-amino derivatives

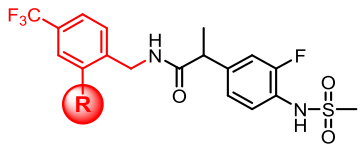

	R	K_i [CAP] (nM)		R	K_i [CAP] (nM)
7	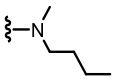	1.2	**18**	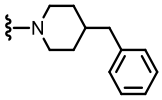	1.4
8	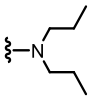	0.3	**19**	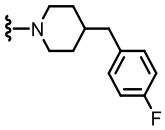	0.4
9		2.3	**20**	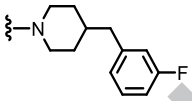	0.4
10		1.7	**21**	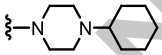	13.8
11		1.6	**22**	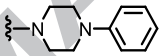	2.0
12	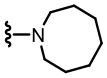	2.8	**23**	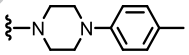	0.7
13	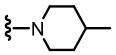	0.9	**24**	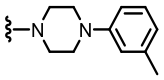	1.8
14	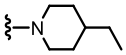	0.7	**25**	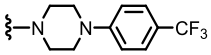	3.9
15	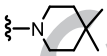	1.3	**26**	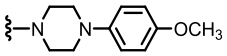	1.6
16	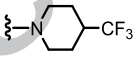	0.4	**27**		7.2
17	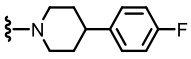	0.9			

Table 2. *In vitro h*TRPV1 antagonistic activities for 2-oxy derivatives

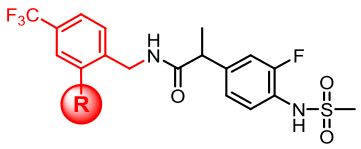

	R	K_i [CAP] (nM)		R	K_i [CAP] (nM)
28		2.0	**33**	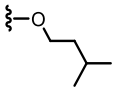	0.5
29	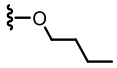	1.0	**34**		0.6
30	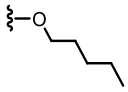	0.7	**35**		0.7
31	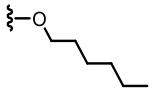	0.8	**36**	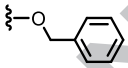	0.9
32		0.8	**37**	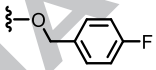	0.5

Table 3. *In vitro h*TRPV1 antagonistic activities for 2-thio derivatives

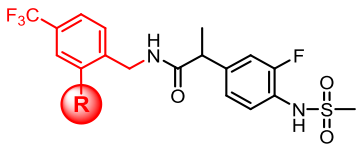

	R	K_i [CAP] (nM)		R	K_i [CAP] (nM)
38	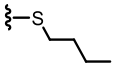	1.9	**44*S***	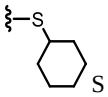	0.3
39	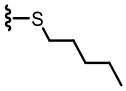	2.3	**44*R***	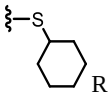	13.9
40	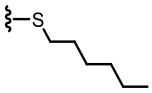	1.8	**45**	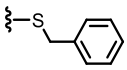	0.5
41	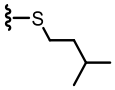	1.4	**46**	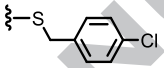	1.1
42	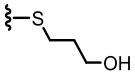	WE	**47**	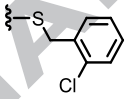	0.9
43		0.3	**48**	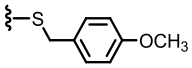	2.3
44		0.5	**49**	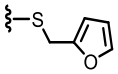	3.2

Table 4. *In vitro h*TRPV1 antagonistic activities for 2-halo, alkyl and aryl derivatives

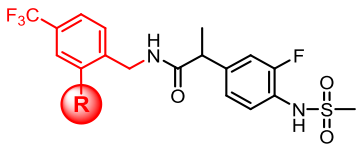

	R	K_i [CAP] (nM)		R	K_i [CAP] (nM)
50		68.7	**57**		1.9
51		4.0	**58**		1.0
52		NE	**59**	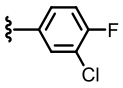	0.6
53	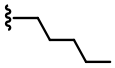	0.4	**60**	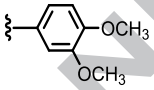	8.6
54		0.6	**61**	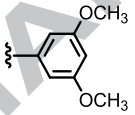	5.8
55	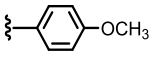	0.8	**62**		59.4
56	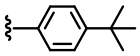	1.1			

Table 5. Comparison of *in vitro h*TRPV1 antagonistic activities for representative, corresponding antagonists from the pyridine and phenyl C-region series

	R	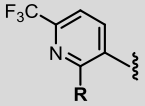	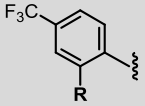
8		0.2	0.3
13	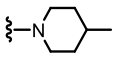	0.3	0.9
16	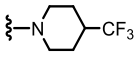	0.4	0.6
18	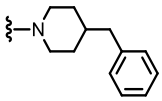	0.2	1.4
33	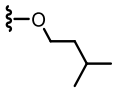	0.8	0.5
34		0.9	0.6
37	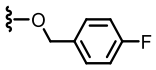	2.5	0.5
43		1.2	0.3
44		0.9	0.5
44*S*		0.4	0.3
47	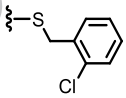	4.9	0.9
53	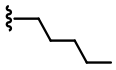	1	0.4
54		0.6	0.6
59	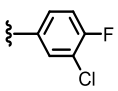	0.2	0.6

Table 6. *In vitro h*TRPV1 antagonistic activities of **43** and **44*S*** for multiple activators.

Activators, parameter	**43**	**44*S***
CAP (f)K_i (nM)	0.3	0.3
NADA (f)K_i (nM)	0.03	0.03
pH, IC_{50} (nM)	32	20.4
heat 45^oC, IC_{50} (nM)	37.2	7.3

Table 7. Inhibition of capsaicin-induced hypothermia after oral administration in the mouse. Data, n = 10, mean ± SEM, * $p<0.05$ vs vehicle.

Dose (mg/kg) /Inhibition %	0.3	3
CAP-induced Hypothermia		
43	38	80
44*S*	NT	57

Figure 2. Analgesic activity of compounds **43**, **44*S*** on CCI-induced cold allodynia (Bennett model) after oral administration in the mouse. Data, n = 10, mean ± SEM, * $p<0.05$ vs vehicle. MPE, maximal possible effect.

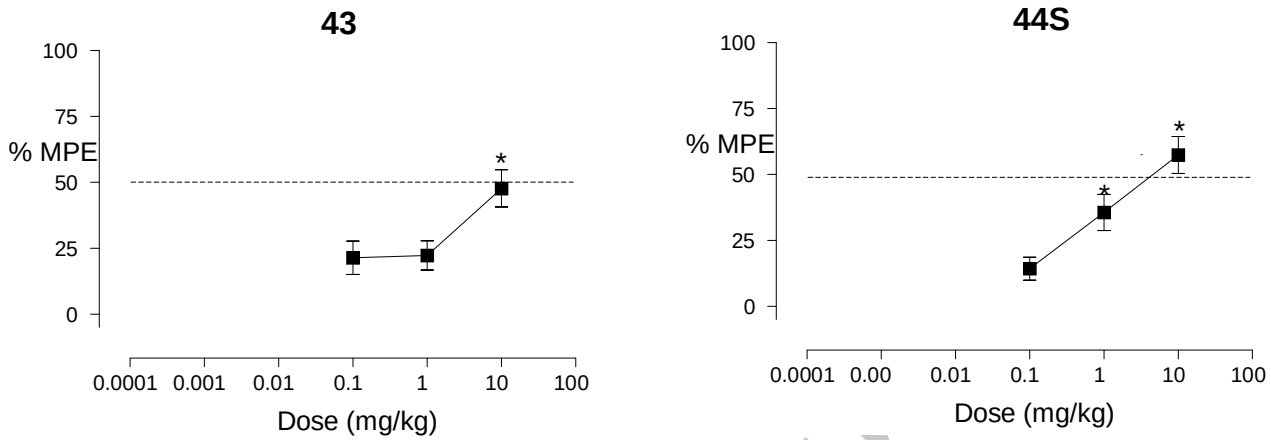

Figure 3. Docking result of **44*S*** in the *h*TRPV1 model.

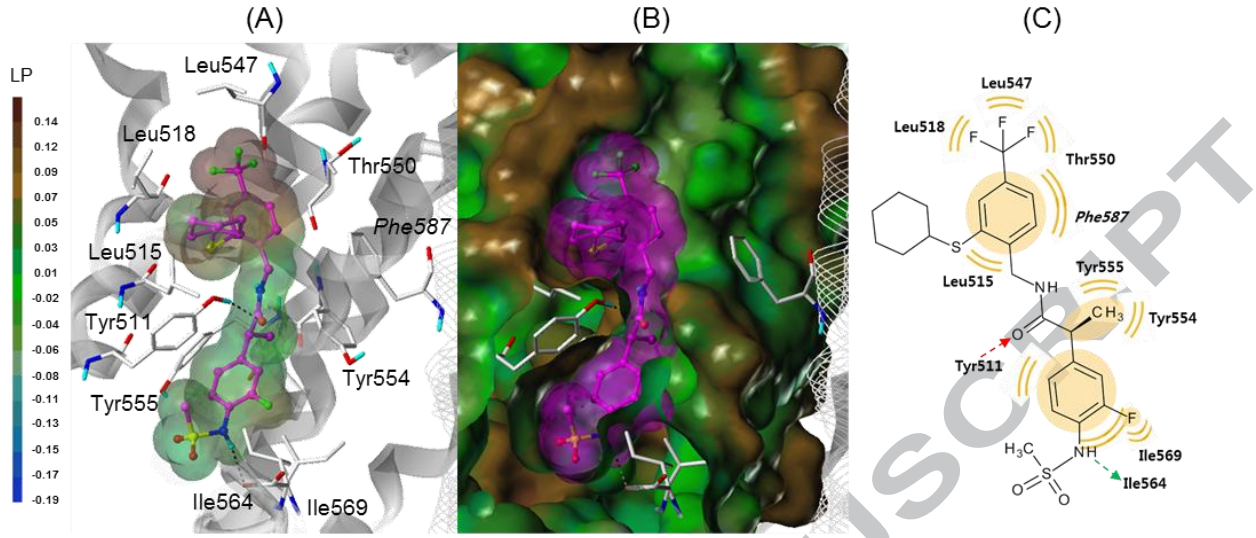

(A) Binding interactions of **44*S*** at the binding site of *h*TRPV1**.** The important interacting residues are labeled and shown as capped-stick with their carbon atoms in white color. The secondary structure of *h*TRPV1 is in gray color and the neighboring monomer helices are depicted in line ribbon. **44*S*** is displayed in ball-and-stick with the carbon atoms colored by magenta. The van der Waals surface of **44*S*** is shown by the lipophilic potential property. Hydrogen bonds are depicted as black dashed lines, and non-polar hydrogens are undisplayed for clarity. (B) The Fast Connolly surface of *h*TRPV1 and the van der Waals surface of the docked **44*S***. MOLCAD was used to generate the molecular surface of *h*TRPV1 and the surface is shown with the lipophilic potential property. For clarity, the surface of *h*TRPV1 is Z-clipped and that of the ligand is colored magenta. (C) 2-D representation of the interactions between **44*S*** and *h*TRPV1. Hydrophobic interactions are marked in light brown. Red and green arrows show the hydrogen bonding interactions with their directionality.

Structure Activity Relationships of Benzyl C-region Analogues of 2-(3-Fluoro-4-methylsulfonamidophenyl)propanamides as Potent TRPV1 Antagonists

Jihyae Ann, Aeran Jung, Mi-Yeon Kim, Hyuk-Min Kim, HyungChul Ryu, Sunjoo Kim, Dong Wook Kang, Sunhye Hong, Minghua Cui, Sun Choi, Peter M. Blumberg, Robert Frank-Foltyn, Gregor Bahrenberg, Hannelore Stockhausen, Thomas Christoph, Jeewoo Lee*

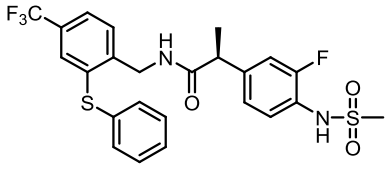

44S
CAP: K_i = 0.3 nM
NADA: K_i = 0.03 nM
pH: IC_{50} = 20.4 nM
Heat: IC_{50} = 7.3 nM